OTC-31064-MS

Pipe Clamping Mattresses to Mitigate Flowline Walking; Physical Modelling Trials on Three Offshore Soils

Colm O'Beirne, Phil Watson, and Conleth O'Loughlin, University of Western Australia; David White, University of Southampton; Alexander Hodson, bp; Sze-Yu Ang and Sebastiaan Frankenmolen, Shell Global Solutions International B.V.; Jesper Hoj-Hansen and Matthew Kuo, Woodside Energy Ltd.; Toby Roe, Subcon

This paper was prepared for presentation at the Offshore Technology Conference held in Houston, TX, USA, 16 - 19 August 2021.

Abstract

Pipe clamping mattresses (PCMs) are a relatively new system for providing anchoring force to pipelines, to mitigate offshore flowline 'walking'. They represent a cost-effective and highly efficient alternative to anchor piles, rock dump and conventional concrete mattresses. The system comprises a hinged concrete structure that clamps onto a section of laid pipeline, with concrete ballast logs securing the clamping action – with the benefit that 100% of the submerged weight of the PCM contributes to axial friction. PCMs have been applied successfully to one deepwater project, but performance data showing the influence of soil type, and allowing a general design framework to be established, has not yet been available.

This paper addresses this gap by investigating the performance of PCMs through three series of centrifuge tests, supported by three Operators. Each series comprises tests on a different reconstituted deepwater soil as follows: (a) West African clay; (b) Gulf of Mexico clay; and (c) carbonate silty sand. In each test, a scaled pipeline is installed in-flight and cycled axially to represent its prior operating life. Scaled PCM models and ballast units are then installed onto the pipe in-flight, mimicking the use of PCMs to mitigate pipeline walking during operation. After installation of the PCMs, further axial cycles are applied, with the system settlement and changes in axial resistance and excess pore pressure measured.

The paper shows the performance and applicability of PCMs for a range of soil types, highlighting variations in axial resistance and settlement. The suite of results will help to calibrate design tools for industry, removing unnecessary conservatism and enabling an optimised pipeline anchoring solution to be designed.

Key results are equivalent friction factors for the combined pipe-PCM system and PCM settlement, which both show behaviour dependent on soil type. In the clay soils, friction increases significantly over time due to 'consolidation hardening'. This provides validation of an important effect that has only recently been recognised in pipeline design. In contrast, hardening behavior is not evident in silty sand – although the study suggests there is potential for increasing resistance associated with settlement, which appears to mobilize additional (wedging) stress around the pipeline. Upon PCM installation, the pipelines embed further due to the added weight. Additional settlement occurs during cycling of the system, due to immediate

soil deformation and consolidation-related compression. The magnitude of embedment is greater for the clay soils, but in all cases does not cause the clamping action to release.

Overall, the efficiency of the PCM system in providing a high level of anchoring force per unit weight placed on the seabed is confirmed. Long term anchoring forces in the range 50-100% of the submerged weight of the PCM are demonstrated. This is several times more efficient than the commonly used alternative of a rock berm.

Introduction

Pipeline axial expansion, buckling and 'walking'

Offshore pipelines experience a longitudinal expansion induced by the high temperature and pressure of the oil or gas being transported during operation. The expansion is resisted by the pipe-soil interface friction resulting in an axial stress along the pipeline, which can then yield vertical (upheaval buckling) or lateral (lateral buckling) translations depending on the path of least resistance.

Over the project lifetime, cycles of operation and shutdown occur at intervals of days or weeks, leading to repeated heating and cooling, with associated cyclic axial displacements. A bias for such displacements in one longitudinal direction over the other often occurs for various reasons including thermal transients (towards 'cold' end), seabed slopes (downhill), a steel catenary riser (towards riser end in tension) and variations in contents density. This can lead to a cumulative displacement in the biased direction colloquially known as axial 'walking' (Bruton 2017).

Subsea pipeline walking is well recognized in design practice e.g. Carr et al. (2006), Bruton et al. (2010). For short pipelines, the entire length can walk but for a long pipeline the walking often feeds into lateral buckles. Although walking is not a limit state for the pipeline itself, it can cause failure at connections to end termination facilities and manifolds, or can lead to excessive bending or axial stress within buckles. The expansion (and contraction), buckling and walking behavior of an offshore pipeline is influenced by the axial pipe-soil interaction. Meanwhile, the axial pipe-soil resistance on clay soils can vary during the life of a pipeline due to consolidation effects associated with the repeated axial movement during startups and shutdowns (White & Bransby 2018). Current pipeline design practice recognises this effect, and considers the potential for both drained and undrained values of axial resistance to apply (White et al. 2017).

Strategies for walking mitigation

Various techniques are used to mitigate walking, some of which are outlined in Table 1. For offshore pipelines in deepwater, excessive cost and potential impact on project delivery schedules are the main drawbacks for implementing such techniques. As such, some pipelines are designed using a 'wait and see' approach, i.e. monitoring for walking and applying mitigating measures only when and where required.

Table 1—Strategies for walking mitigation

Method	Description	Main shortcoming
Conventional concrete mattresses	Modular concrete mat laid over pipeline providing added vertical stress and thus increased axial resistance.	Potential for arching if pipe embeds deeper
Rock-dump	Rock berm with sloping sides over pipe providing added vertical stress and thus increased axial resistance.	
Hold-back anchors	Anchors installed at the ends of the pipeline or (for longer pipelines) at various locations along its length. May include suction buckets, piles, skirted foundations/mudmats, hybirds of mudmat and pin piles.	Expensive and complex installation/ tethering
Trenching	Laying pipe in seabed excavation. Can include conventional excavating, dredging, plowing or jetting. Typically uneconomical for deep offshore and potentially detrimental for any other (future) applications of walking mitigation.	Must be incorporated at time of pipe-lay

Trenching is predominantly used to control excessive buckling and must be incorporated at the time of pipe-lay – and so is not suitable for a 'wait and see' approach. Hold-back anchors, together with an appropriate tethering system, can be very expensive and complex to install in deepwater (Perinet & Frazer 2006). Accordingly, conventional concrete mattresses and rock-dump are often preferred. However, mitigation of axial walking depends on the active stress applied by these anchoring techniques. Recognizing the tendency for a pipeline to embed deeper into the seabed with axial displacement cycles (White et al. 2011), concrete mattresses can be prone to arching thereby compromising the available axial restraint. Likewise, for rock dump, recent studies by Carneiro et al. (2017), Rodriguez et al. (2018) and O'Beirne et al. (2021) have reported the potential for stress redistribution within rock berms resulting in arching over the pipe crown, a reduction in pipe/rock contact area and ultimately a loss of effectiveness to arrest walking.

Pipeline clamping mattress

Pipe clamping mattresses (PCMs) are a relatively new system developed by Shell, and have been successfully used to mitigate offshore pipeline walking. The PCM concept is subject to patent application, and was first publicised at OTC in 2017 in Frankenmolen et al. (2017). PCMs comprise a hinged concrete structure of two matching (mirrored) reinforced precast slabs as illustrated in Figure 1. The slabs are connected by structural wires (installed internally to tight tolerances prior to concrete pouring) to form the hinge which tracks axially along the pipeline. Log mattresses provide ballast on top of the lower clamp, increasing the grip of the PCM onto the pipe.

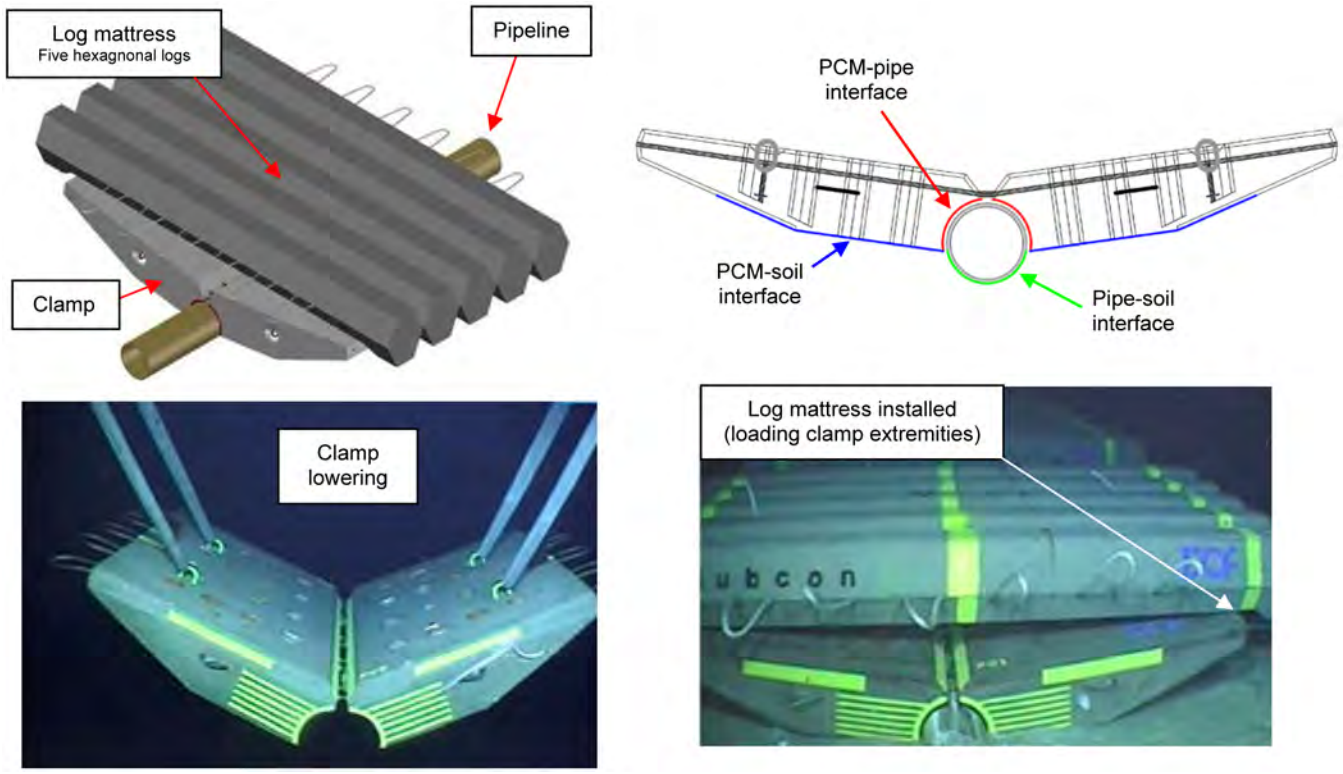

Figure 1—Pipe-clamping mattress (adapted from Frankenmolen et al. 2017)

The geometry of the PCM is designed such that the full submerged weight of the clamp and mattress is firmly attached to the pipe, and bears onto the seabed either directly or through the pipe. As a result, the full PCM weight enhances the seabed friction that must be overcome for the pipe (and PCM) to move axially on the seabed. The PCM therefore represents a highly efficient alternative to rock-dump and concrete mattress options, where only part of the submerged weight contributes to axial resistance.

The clamping surfaces feature a rubber layer (to assist the clamping action), and where in contact with the seabed, drainage holes in each slab promote faster soil consolidation. Lifting points on the clamp are used to manoeuvre it over the top of the laid pipe for installation. By capitalising on the hinged assembly, it naturally self-aligns and clamps onto the pipe during lowering. Following deployment, a conventional precast concrete log mattress is installed over the clamp, with its weight acting on the outer extremities of the clamp to maximise the leverage and secure the clamping action.

PCMs have been successfully used for the Malampaya deepwater gas project as reported by Frankenmolen et al. (2017). In this case, prior to PCM deployment, pipeline axial displacement was reportedly reaching about 28 mm per shutdown and restart cycle and had accumulated to a displacement of 1.8 m (over almost 200 cycles) at the Pipeline End Structure. A total of 15 PCMs were installed over 5 pipe joints in 2015 - each PCM having a dry weight of around 16 tons and dimensions of 4 m (along the pipe) by 2.75 m in plan (see Figure 1). Monitoring has shown that the PCMs have been effective at stopping the walking.

Scope of study

The success of the PCM concept at Malampaya has led to interest in its application for other soil types and pipelines. The technology could justify adopting a 'wait and see' approach for new projects, where there may be design uncertainty regarding the potential for pipeline walking. In other cases, PCMs may be added as necessary to existing pipelines.

The original PCM geotechnical design was based primarily on analyses extrapolated from pipeline-seabed interaction, supported by a standard suite of classification and interface tests. Physical modelling was not carried out and performance data showing the influence of soil type was not yet available. The current study investigates the performance of PCMs through three series of centrifuge tests, supported by three Operators. Each series comprises tests on a different reconstituted deepwater soil as follows: (a) West African clay; (b) Gulf of Mexico clay; and (c) carbonate silty sand. An earlier introductory paper briefly showcasing the testing approach in one soil type (O'Beirne et al. 2020) has previously been published.

The modelling addresses two knowledge gaps related to PCMs in different offshore soils as follows:

1. Quantifying the *short and long-term (hardened) friction coefficients*, and the time and number of cycles for the transition process; and
2. Quantifying the *settlement of the PCM-pipe system* and investigating the *robustness of the clamping arrangement* in response to this settlement.

The suite of results will ultimately help to calibrate design tools for industry, removing unnecessary conservatism and facilitating optimised pipeline anchoring solutions.

Paper structure

The three offshore soils and technical details of the physical modelling performed are first described. The apparatus, procedures and overall test programme are then outlined. An example of a typical test output together with an overview of interpretation is discussed. The overall results and key observations from each of the test programmes are then presented. Finally, an overview of the PCM performance along with some concluding remarks are given.

Centrifuge modelling with three offshore soils

Centrifuge modelling advantages

The strength and stiffness of soil are governed by effective stress, so small-scale model tests at unit gravity do not capture the correct behaviour. When a small-scale model is accelerated within a centrifuge, the self-weight of the soil is enhanced by the ratio of the centrifuge acceleration to Earth's gravity. This ratio is

denoted n, and is the scaling factor required to convert dimensions of a centrifuge model to the dimensions of the corresponding field scale situation. Obtaining similitude between the model and field stress (and strain) conditions allows realistic performance data to be gathered. For this study the stresses applied to the seabed from the weight of the pipe and PCM are scaled correctly. Furthermore, the centrifuge environment accelerates consolidation processes (by a factor n^2 versus an equivalent prototype). This allows long-term field scale events (in this case the 'whole life' loading histories of PCMs in fine-grained soils) to be replicated within a practical test period (White 2020).

The National Geotechnical Centrifuge Facility (NGCF), at the University of Western Australia was engaged to perform tests with the various offshore soils to tackle the main PCM knowledge gaps using realistic small-scale models. The 10 m diameter fixed beam centrifuge was used for all three series (Gaudin et al. 2018).

Offshore soils and sample preparation

The study reflects a multi-operator testing campaign for real-world applications across three different deepwater projects, with three different seabed soils as follows:

- Two clays; one from offshore West Africa (denoted 'WAf') with a liquid limit (LL) of 85% and plasticity index (PI) of 40%, and one from the Gulf of Mexico (denoted 'GoM') with LL = 94% and PI = 66%. Both clays were entirely fine-grained, with 100% passing the 75 μm sieve.
- A coarser carbonate material of 'silty sand' by USCS definitions ('sandy silt' by Australian Standards) was also investigated (denoted 'SS'). The material comprised >90% calcium carbonates typical of many offshore sites, 50-60% fine-grained sand (sub-angular to angular, poorly graded), 40-50% fines and traces of gravel. Hydrometer testing showed the fines portion to be mostly silt-size, with a LL = 40% and a low PI < 10%.

Each soil was reconstituted to model the seabed in the three centrifuge test series. Although the details of the reconstitution process varied slightly between each soil, it typically involved the following steps:

1. Mixing the soil to a specified water content.
2. Preparing a rectangular strongbox (0.39 m width × 1.3 m length × 0.225 m depth) with a 20 mm sand drain at the base, overlain by a permeable drainage mat.
3. Transferring the soil into the strongbox, aiming to minimise the entrainment of air.
4. Performing initial stages of consolidation/compaction.
5. Installing small diameter PVC pipes in two (diagonally opposing) corners to ensure a hydraulic link between the top and bottom drainage layers, and prevent any hydraulic gradient across the sample height.
6. Consolidating in-flight under self-weight at g, together with a surface surcharge (for the clays).
7. Monitoring sample settlement and, when excess pore pressure dissipation was considered essentially complete, performing penetrometer tests to characterise the sample strength.

The final sample heights were between 110 and 120 mm, which is believed to be sufficient to avoid (base) boundary effects considering the nature of the surface testing. Some additional variables for each of the soil reconstitution processes are given in Table 2.

Table 2—Soil sample preparatio

	WAf	GoM	SS
Pre-consolidation sample preparation	wc = 300%, mechanically mixed for 24 hours	wc = 160%, mechanically mixed for 24 hours	wc = 45%, mixed by hand and trowel for ~2 hrs (see note 1)
Soil transfer to strongbox	Carefully poured into strongbox, aiming to minimise the entrainment of air		Placed by hand into strongbox in 30 mm lifts
Initial consolidation/ compaction	Consolidation press at 10 kPa	Consolidation press at 5 kPa	After each lift, compaction via falling weight (see note 2)
Centrifuge acceleration, *n*	30g		21.35g
Centrifuge consolidation details	10 kPa surcharge (see note 3)	6.7 kPa surcharge (see note 3)	No surcharge

Notes:

1. Throughout the mixing process carbonate particles greater than sand size (i.e. shells > about 2.5 mm) were removed.
2. Comprised 10 to 15 blows of a 2 kg weight with drop height ~ 180 mm. The energy of the falling weight acted over a square 205 mm wide base plate which was repositioned across the sample to cover its entire surface area (incorporating ~20 mm overlaps). Excess surface water pooling was removed by soakage after compaction of each lift.
3. After consolidation under the surcharge stress, the surcharge was removed, and the sample allowed to swell prior to testing.

In-flight soil characterization

In-flight penetrometer tests were performed to assess the sample characteristics. For the clays, a miniature T-bar penetrometer was used, and the resulting strength profiles are shown in Figure 2a. Both clay profiles showed a linear increase in strength with depth, beyond z ~ 0.5 m. At shallower depth the strength reduces towards zero at the mudline. The WAf clay had approximately twice the strength of the GoM clay. Piezocone dissipation tests in the clays indicated a consolidation coefficient of ~2 m²/year.

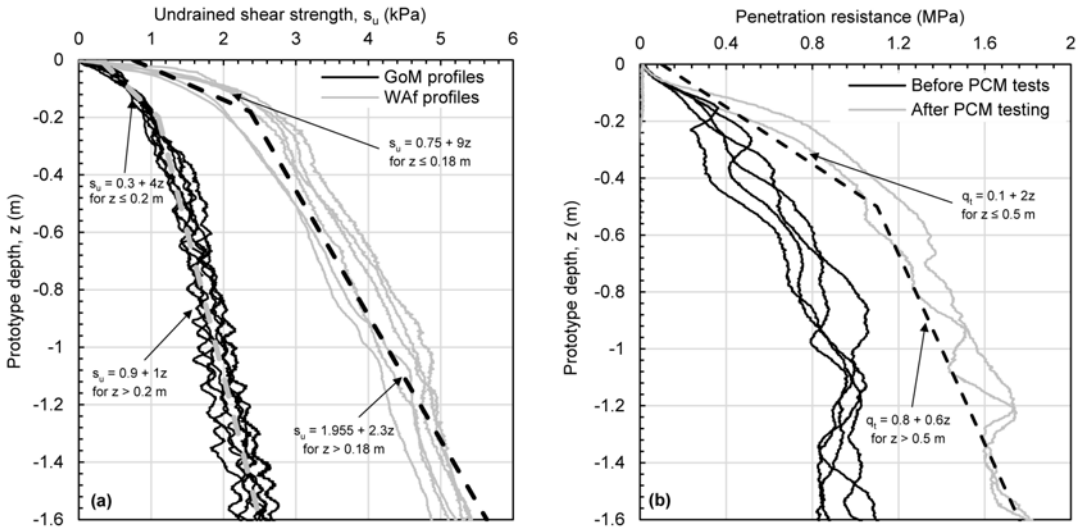

Figure 2—In-flight penetrometer results: (a) undrained shear strength profiles in clays as determined by T-bar testing; and (b) penetration resistance in silty sand as determined by CPTs

A miniature cone penetrometer was used in the SS sample. Penetrometer tests carried out soon after the PCM and pipeline testing indicate some strength increase ('hardening') with time over the full depth of the sample, potentially due to continued soil compaction under self-weight at g (and as a result of repeated cycles of ramping up and down the centrifuge). The post PCM penetrometer results best reflect the sample strength during PCM testing (the pre-test penetrometers being conducted well in advance of the PCM tests). The cone tip resistance increased from near zero at mudline to approximately 1 MPa at z = 0.5m, and then increased at a gradient of ~0.6 MPa/m (Figure 2b)

Interface shear box tests

Low-stress interface shear box tests (ISBs) were carried out to explore the friction coefficients of the pipe-soil and PCM-soil interfaces. Four to six ISBs were completed for each of the different soils. For the clays, both the undrained (shearing rate = 0.1 mm/s) and drained (shearing rate 0.001 mm/s) responses were considered while the SS testing focused on the drained response. The effect of remoulding and overconsolidation ratio (OCR) on interface strength was also explored for the clays.

The ISB interface material comprised aluminium plates mimicking the pipe/PCM material (i.e. anodized and sand blasted as necessary to accurately reflect the model surface roughnesses) and the shear cycling was episodic. A summary of the results (corrected for apparatus friction) is given in Table 3 where averages of the forward/back friction coefficients (shear stress ratios) for various cycles are given.

Table 3—Interface strength parameters from planar testing

Soil parameter	WAf	GoM	SS¥
Normally-consolidated undrained interface strength ratio, $(s_u/\sigma'_{no})_{nc}$	0.38* - 0.62†	0.22* - 0.30†	-
Effect of OCR on undrained strength: value of (s_u/σ'_{no}), at specified OCR	0.54* - 0.79†(for OCR = 2)	0.39* - 0.52†(for OCR of 3)	-
Drained interface strength ratio, (τ/σ'_n)	0.74‡ - 0.95§	0.42‡ - 0.62§	0.40 - 0.43, Smooth interface 0.60 - 0.65, Rough interface

* At end of second cycle pair

† At end of last cycle pair following episodic consolidation

‡ OCR = 1

§ OCR = 2 or 3

¥ Also confirmed with additional centrifuge tests (in-flight strip surface drag tests)

Models and arrangement

Variations for real-world projects

The same pipe OD and PCM sizes were investigated at both clay sites, while the pipe OD and PCM submerged weight at the silty sand site were about 30% lower. The PCMs clamped along a 3.5 m span of pipe. Both clay test series were carried out at a centrifuge acceleration of n = 30 and the silty sand series at n = 21.35. Key details are provided in Table 4 and Table 5 for the different test series in prototype units, with dimensions scaled down by n and loads scaled down by n^2 for the modelling.

Table 4—PCM key details

PCM key detail	Unit (prototype scale)	WAf	GoM	SS
Clamp submerged weight, (normal; light)	kN	77.85; 41.76		47.66; 25.7
Model surface roughness, Ra1	µm	4.2 - 4.5	5.2	3.8
Length along (parallel to) pipe	m	3.5		3.5
Width perpendicular to pipe (if flat)	m	4.47		3.25
Height	m	0.5		0.45
Log mattress submerged weight, (normal; light)	kN	97.0; 49.42		71.87; 35.66
Total length along (parallel to) pipe	m	3.33		3.33
Length perpendicular to pipe	m	5.2		3.8

* Roughness given at actual scale, as measured on model

Table 5—Pipe key details

Pipeline detail	Unit (prototype scale)	WAf	GoM	SS
Pipeline OD	m	0.51		0.363
Submerged weight, (normal; alternates)	kN/m	1.03; 1.9	1.03; 0.73	0.51; 1.05; 2.14
Model surface roughness, Ra[1]	μm	5.2	4.0; 5.1	1.77

Model PCMs

The model PCMs were primarily fabricated from aluminium, sand blasted and anodised to ensure a rough contact surface with the soil. The clamp component featured a loose pin butt hinge to allow for precise clamping around the model pipeline, with silicone strips along the clamping surfaces as shown on Figure 3. In its fully closed (clamped) position around the pipe, the rise angle was typically around 7° from horizontal (Figure 3a). Voids milled into the clamp allowed for its submerged weight to be varied. Various plastic insert pairs of different mass could be tightly fitted to achieve 'normal' and 'light' weights. The model clamps featured hoist holes and 16 base drainage holes with porous plastic discs fitted into circular recesses. The drainage holes were tested under atmospheric pressure to confirm their functionality before and after the centrifuge tests.

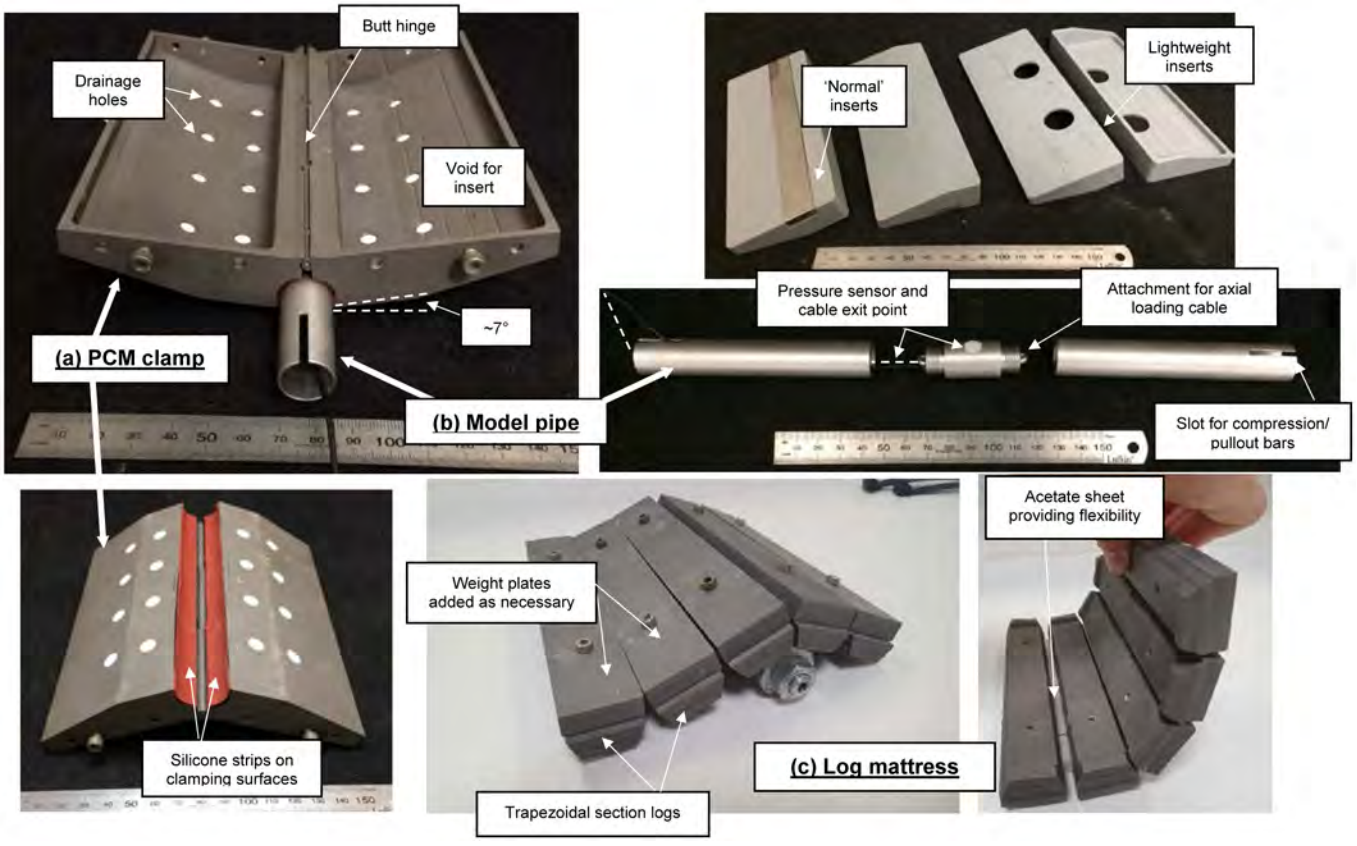

Figure 3—Model PCM and pipe

Each model log mattresses comprised five aluminium 'logs'. While the prototype logs are a hexagonal shape (see Figure 1), a trapezoidal cross-section (elongated lower-half hexagonal) was used for the models, allowing weight strips to be attached/removed to achieve the 'normal' and 'light' target weights (Figure 3b). The plate widths were scaled directly from the width across corners of the prototype hexagonal shape

to correctly model the gaps between the logs. An acetate sheet was fastened between the model logs and the weight plates to connect the logs while providing flexibility across the mattress.

Model pipes and instrumentation

All model pipes were fabricated from aluminium, comprising three sections (as shown in Figure 3), which screwed together to form overall lengths greater than 10 diameters. A 'double length' pipe was also investigated in the GoM testing to consider the influence of end effects. Pipes used for the clay sites were sand blasted to mimic rough polypropylene coatings, while a smoother interface was adopted for the silty sand tests. All pipes were anodised to prevent damage during the submerged tests.

The substantially solid central section housed a transducer to capture the development and dissipation of excess pore pressure at the invert during testing. Cables were connected at attachment points at either end of the central section. These cables extended to a loading frame, through which axial movement was applied to the pipe. Two load cells mounted between the cable and the frame measured the axial loads. The two end sections had a wall thickness of ~1 mm. To meet the required in-situ submerged weights, 3D-printed hollow buoyancy 'boosters' (watertight plastic boxes) were used as required.

Test arrangement

While some changes were incorporated across the different test series, the principal approach is captured in Figure 4. A loading frame, connected to the actuator via an adaptor, comprised a beam with an assortment of detachable members. These members included elements to allow the pipe to be pushed (and cycled) into the seabed to target a specific installation depth (these are then removed to 'free' the pipeline for axial cycling); a frame to apply axial displacement to the pipe via a stainless steel wire cable that incorporated a small load cell; and guides to stop the pipe rotating without creating additional friction.

Non-contact (laser) displacement sensors were used to measure the axial displacement and pipe settlement. The position of the vertical axis of the actuator (and hence the I-beam) was controlled through a feedback loop, to ensure the orientation of the cable pulling the pipe remained horizontal as the pipe settled. Four wire cables were connected to a secondary linear actuator allowing the PCM to be suspended in an open (unclamped) position over the pipeline prior to lowering in-flight.

Test procedure and example results

Each of the three centrifuge test series comprised five to six model tests typically covering variations in pipe and PCM submerged weight, model pipe length, consolidation period and sequencing of axial cycling. Pipe 'over-exposure' in the silty sand, through the removal of soil adjacent to the pipe, was also considered (to relieve wedging stresses) which is explained later in this paper.

In each case the pipe was pushed to a targeted initial embedment of 0.3D, with 10 vertical cycles (between mudline and 0.3D) applied at a (model) displacement rate of 0.5 mm/s, sufficient to achieve an undrained response in the clays. The centrifuge was then ramped down to remove the tension/compression supports (thus releasing the pipe), before being promptly ramped back up and left for an extended period (prototype times given on Table 6) to dissipate excess pore pressure around the pipe.

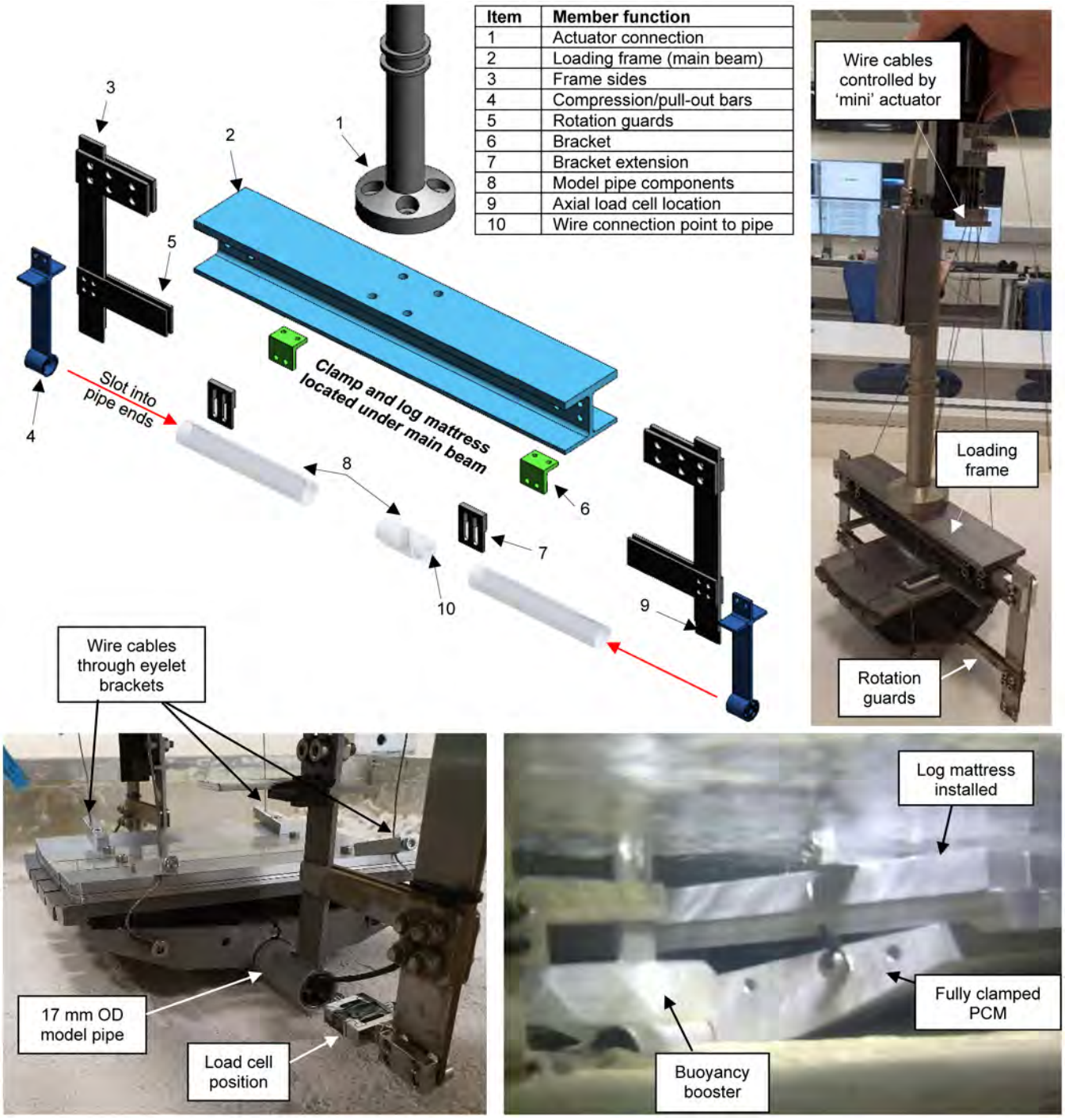

Figure 4—Pipeline loading apparatus and components

Table 6—Test matrix for Stage 1 (pipe-only)

Test ID	Pipe	Initial embedment depth (D)	Time before axial	Cyclic axial amplitude cycles (D)	Axial cycles	Consolidation times following cycle sweep	
						Outward	Inward
GoM-1	N[1]	0.3 (with vertical cycles)	~ 2 months	0.5	15	~ 30 mins	~ 1 week
GoM-2					15		
GoM-3					17		
GoM-4	Long				15		
GoM-5					15		
WAf-1	N			0.5	15	~ 45 mins	
WAf-2				0.25			
WAf-3				0.125	17		
WAf-4				0.5	15		
WAf-5							
WAf-6							
SS-1			~ 2 weeks to 1 month	0.5	22	~ 30 mins	~ 1.5 days
SS-2					21		
SS-3					22		
SS-4					23		
SS-5					22		
SS-6[2]					22		

Notes:

1. 'N' = normal (base case).
2. SS-6 featured sediment removal either side of the pipeline following vertical cyclic installation (i.e. while the pipe was still rigidly connected to the loading frame and before Stage 1 axial cycles) to simulate over exposure of the pipeline, prior to PCM installation. This involved scraping a 1V:5H slope from the bottom of the pipe up to the existing mudline level (on both sides of the pipe).

Following pore pressure dissipation, each test comprised the following two main stages (annotated data from a typical test in clay is provided in Figure 5):

- Stage 1: This stage represents the operating life of the pipeline prior to PCM installation, with cyclic axial movements caused by heating and cooling. An initial series of 'pipe only' axial cycles with the pipe displaced typically by a limit-to-limit distance of 0.5D for (typically) 15 or 22 cycles in the clays and silty sand respectively. Individual cycles occurred at weekly intervals for the clays and 1.5 days for the silty sand, with only a brief pause between outward and inward sweeps. Smaller axial displacements were also investigated for two of the West Africa tests as listed in Table 6.
- Stage 2: This stage represents the PCM installation and subsequent axial loading cycles. The PCM clamp was lowered onto the pipe, followed by a 1 or 2 week pause (reflecting sequential offshore activities), after which the log mattress was lowered onto the clamp. After a predetermined pause period (ranging from 1 week to over 1 year), Stage 2 typically involved cyclic 'packets' of axial movement, with each packet comprising four small cycles (sweeps of 0.125D) followed by one large cycle (sweeps of 0.5D). This variation in movement distance is a simple representation of an uneven sequence of operating temperatures due to partial and full shutdowns. These varying amplitudes were not incorporated in the West Africa clay (and one of the silty sand tests) where instead the sweep displacement was kept constant as shown in Table 7. A range of times was allowed between individual cycles with the overall intent to closely represent actual pipeline

conditions. Approximately 1.5 days however was considered sufficient for the more drained silty sand response.

Table 7—Test matrix for Stage 2 (pipe + PCM)

Test ID	Pipe	Clamp and log mattress	Consolidation times following			Cyclic axial amplitude (D)	Axial cycle packets[3] or * *total cycles*	Consolidation times following cycle sweep	
			Stage 1 cycles (weeks)	Clamp installation (weeks)	Log mattress installation			Outward	Inward
GoM-1	N[1]	Light	~ 1	~ 1	~ 1 week	Small = 0.125 Large = 0.5	10	~ 30 mins	~ 2 weeks
GoM-2					~ 1 year		13		
GoM-3		N					12		
GoM-4	Long						8		
GoM-5					~ 4 weeks		*8		
WAf-1	N	N	~ 1	~ 1	~ 1 week	0.5	*25	~ 45 mins	~ 1 week
WAf-2					~1.5 months	0.25	*17		~ 1.5 months
WAf-3					~ 1 week	0.125	*72		~ 1 week
WAf-4					~1.5 months	0.5	*30		~ 1.5 months
WAf-5		Light			~ 1 week		*76		~ 1 week
SS-1	N	N	~ 2	~ 1	~ 1 week	0.5	*130	~ 30 mins	~ 1.5 days
SS-2						Small = 0.125 Large = 0.5	6		~ 15 days
SS-3[2]							31		~ 1.5 days
SS-4		Light					39		

Notes:

1. 'N' = normal (base case).
2. SS-3 featured sediment removal either side of the pipeline following Stage 1 (i.e. before installing the PCM and log mat) to simulate over exposure of the pipeline. This involved scraping a 1V:5H slope from the bottom of the pipe up to the existing mudline level (on both sides of the pipe).
3. A cyclic packet comprises 4 small cycles (0.125D amplitude) followed by 1 large cycle (0.5D amplitude) with the same consolidation times applied between cycles. Tests in the West Africa clay, together with GoM-5 and SS-1 (i.e. those marked with an asterisk in the table) did not feature cycle packets, but instead were completed at a constant amplitude.

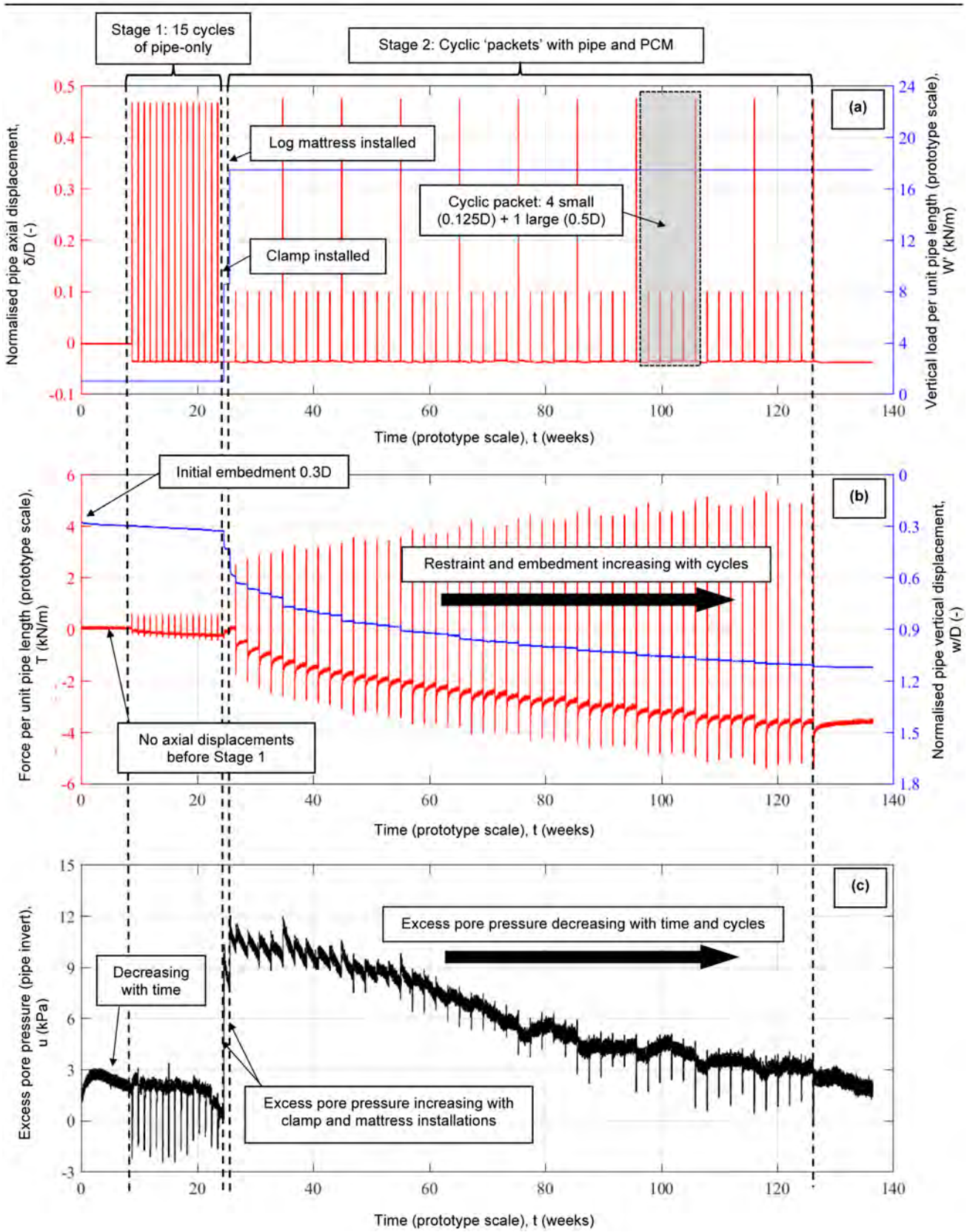

Figure 5—Typical PCM test data (GoM-1)

A full set of typical test result time histories are shown on Figure 5, from test GoM-1. In this test a short (1-week) pause was incorporated between lowering of the log mattress and the start of Stage 2 axial cycling. A further 2-week pause was included between each 'pipe plus PCM' cycle.

The controlled test parameters are shown on Figure 5a, being (i) the axial pipe and pipe/PCM displacement, δ/D (shown in red) and (ii) the current on-bottom weight of the pipe and pipe/PCM (shown in blue). This weight is expressed as the submerged weight per unit pipe length, W′ (so the PCM weight is normalised by the length of the model pipe).

The pipe embedment, denoted w/D on Figure 5b (shown in blue), increases during Stage 1 cycling, but by a minimal amount. Once the PCM clamp is added, immediately followed by the log mattress, (increasing the vertical load on the pipe), a notable increase in the embedment of the system occurs. The vertical total stress increase from the PCM weight generates excess pore pressures at the pipe invert in the clay soil (Figure 5c). System embedment gradually increases throughout the Stage 2 axial cycling, with excess pore pressures gradually dissipating. These changes are accompanied by a gradual increase of axial resistance (denoted T, and reported per unit pipe length, shown in red on Figure 5b), reflecting consolidation hardening, as observed in similar full scale model tests (e.g. Smith & White, 2014) and numerical simulations (Yan et al. 2014).

The test results are shown as the axial force-displacement response in Figure 6. Figure 6a shows the axial force throughout the full test, including stages 1 and 2. Every 5th (or 10th) cycle is highlighted in colour to illustrate the test progression more clearly. Figure 6b and Figure 6c present the response as the axial friction factor (T/W′) with the key cycles in Stages 1 and 2 highlighted, respectively.

The axial resistance generated during the pipe-only cycles is dwarfed by the axial resistances with the PCM installed, highlighting the influence of the PCM weight (Figure 6a, see also Figure 5b).

For Stage 1 (the first 15 cycles), W′ is the pipe weight alone, whereas W′ is the pipe plus PCM weight for Stage 2. The friction factor normalisation leads to comparable values of T/W′ for both stages. The pipe-only cycles show a progressive doubling in friction factor (hardening) to T/W′ ~ 0.38 by the 15th cycle. However, the initial (cycle 1) outward sweep is notably greater than its corresponding inward sweep. Also, notable peaks in friction factor occur at the start of the pipe-only outward sweeps. These and other observations are discussed further in the results section.

After the PCM is installed, a relatively low friction factor of T/W′ ~ 0.11 is initially observed compared to that developed during the pipe-only cycles. This reflects a rise in excess pore pressure under the weight of the PCM (i.e. undrained material response and lower effective stress). Nevertheless, this still translates to significantly higher axial resistance compared to the pre-PCM condition as outlined earlier.

With continued cycling and excess pore pressure dissipation, T/W' rises to ~ 0.30 at the end of the test, but has not yet stabilised. Representative cycle-by-cycle 'residual' friction factors are shown in Figure 7 to illustrate this hardening behaviour. The data points are averaged over a small displacement interval towards the end of the outward and inward sweeps, with the average of both sweeps then taken as the 'average' cycle value.

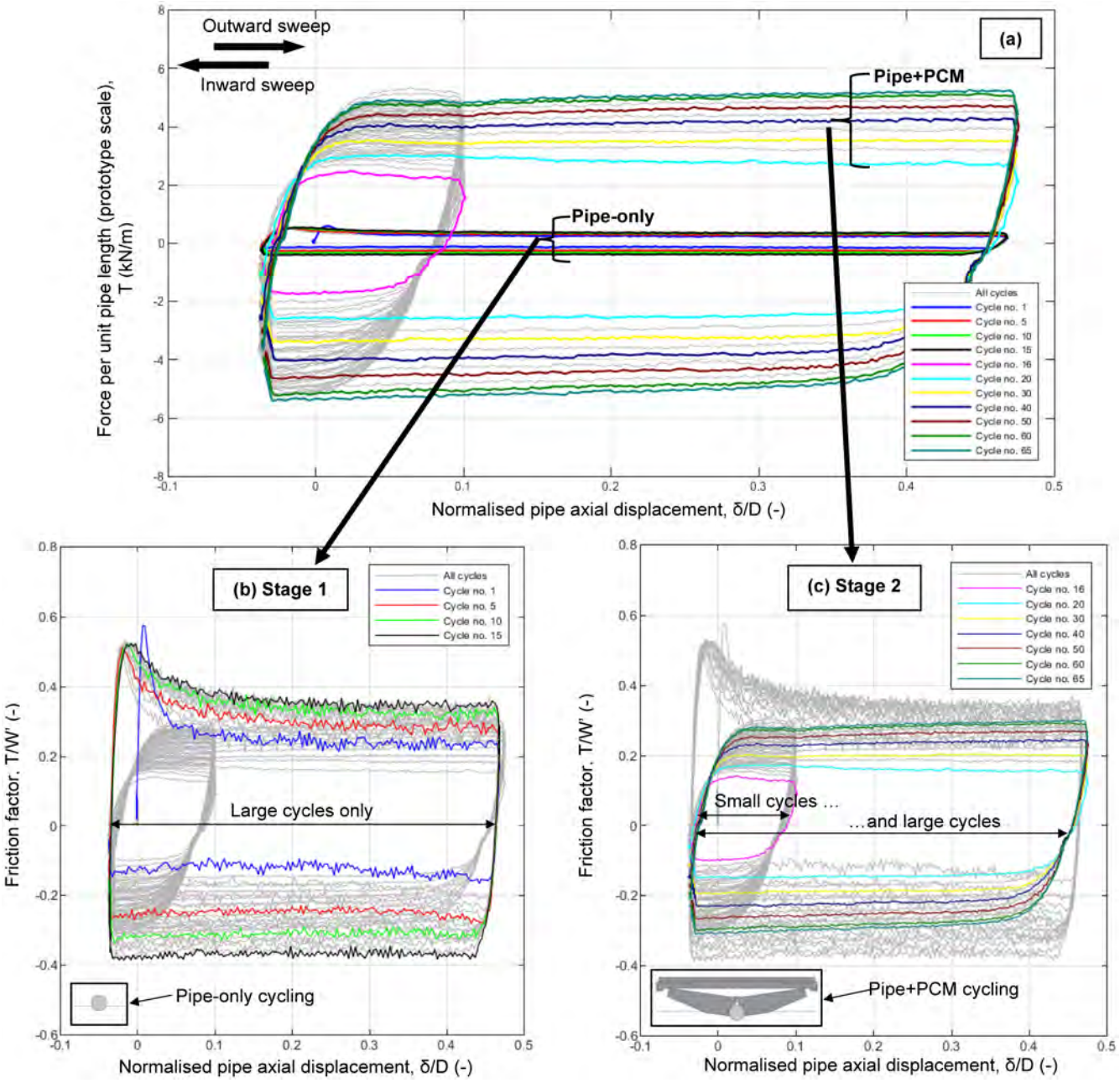

Figure 6—Typical friction factor development in clay (GoM-1)

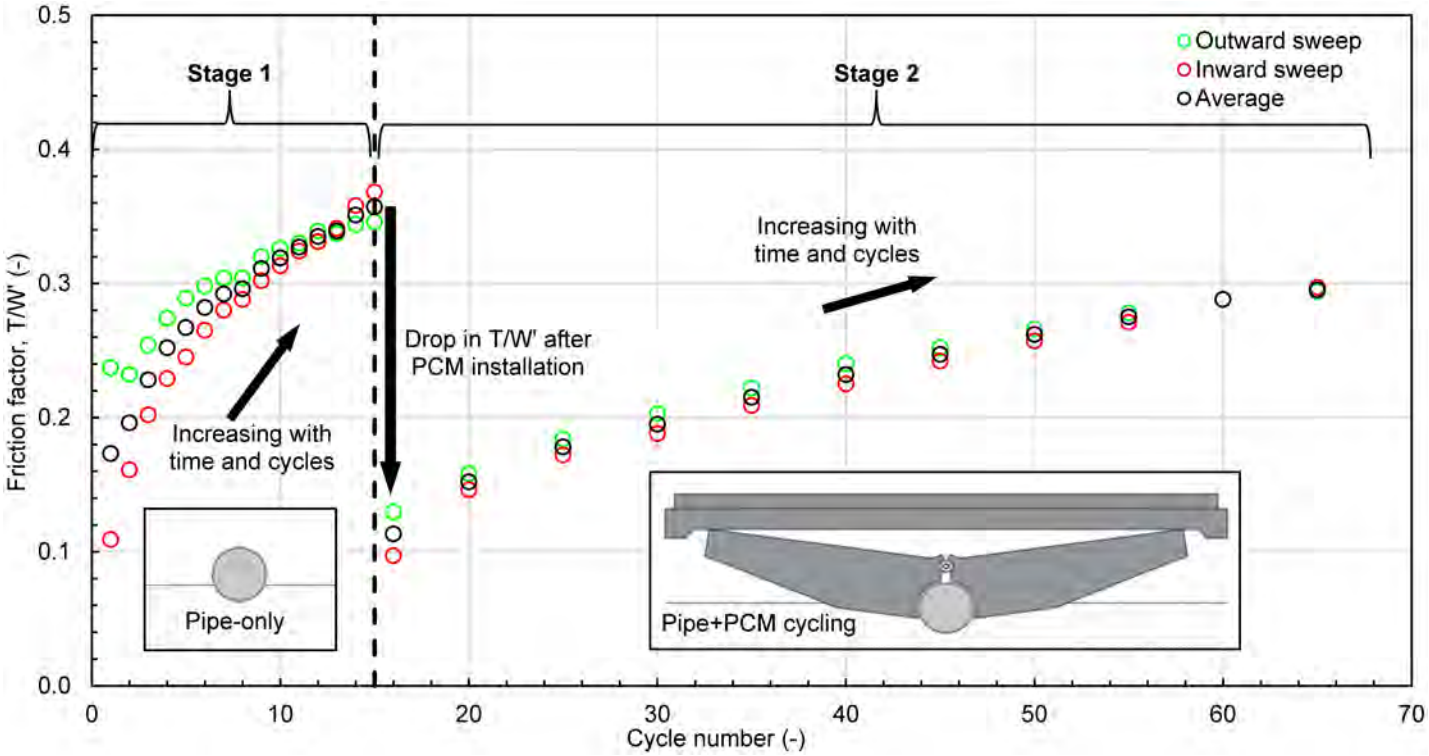

Figure 7—Residual friction factor development in clay (GoM-1)

Results and observations – clay

Overview of GoM test series observations

The cycle-by-cycle measurements of friction, excess pore pressure at pipe invert and pipe embedment, from all of the GoM tests are summarized in Figure 8. Observations from the friction response are:

1. The initial friction factors for the 'pipe-only' test stages are in the range 0.16 - 0.21. This friction increases with axial cycles of the pipe, approaching the drained capacity. By cycle 15, these friction factors are generally in the range 0.36 - 0.4. Slightly higher friction values (e.g. in GoM-5) may correlate with higher initial pipeline embedment, reflecting wedging effects.
2. After installing the PCM, the initial friction factors are generally in the range 0.14 - 0.20 over the first large displacement axial cycle (typically cycle #20). As with the 'pipe-only' test stage, the friction gradually increases over the course of each test, with values of 0.23 to 0.30 recorded for cycle 50, i.e. typically a 50% increase compared to the first large cycle after PCM installation. This rise in friction appears to be ongoing at the end of each test, so the steady state friction would be higher than these measured values, and therefore closer to the friction factors measured for the 'pipe-only' stage (as drained conditions are approached).
3. Tests with long (~ 1 year) consolidation periods following PCM placement (i.e. GoM-2, 3 and 4) yield much higher friction over the very first small (0.125D) axial cycle, when compared to tests with a shorter (1 and 4 weeks) consolidation period (i.e. GoM-1 and GoM-5). However, the comparatively higher frictions are quickly lost with further axial cycling of the pipeline.
4. Similar initial friction factors for the 50% and 100% weight PCMs (i.e. GoM-2 and GoM-3 respectively) are observed during early cycles after PCM placement. However, the 100% weight system seems to trend towards a lower friction value, which could be linked to a stress level effect on soil friction angle, but perhaps also influenced by higher excess pore pressures and embedment.

5. The long pipe setup (i.e. GoM- 4) yielded comparable (albeit slightly lower) initial friction to that of the equivalent short pipe test (i.e. GoM- 3) during early axial cycles after PCM placement. The friction increases faster with cycles but seems to plateau to ultimate values that are like the comparable short pipe tests. The early disparity could be due to a slightly less embedment of the system with the long pipe (which provides a greater bearing area), and hence less excess pore pressure generation and faster consolidation.

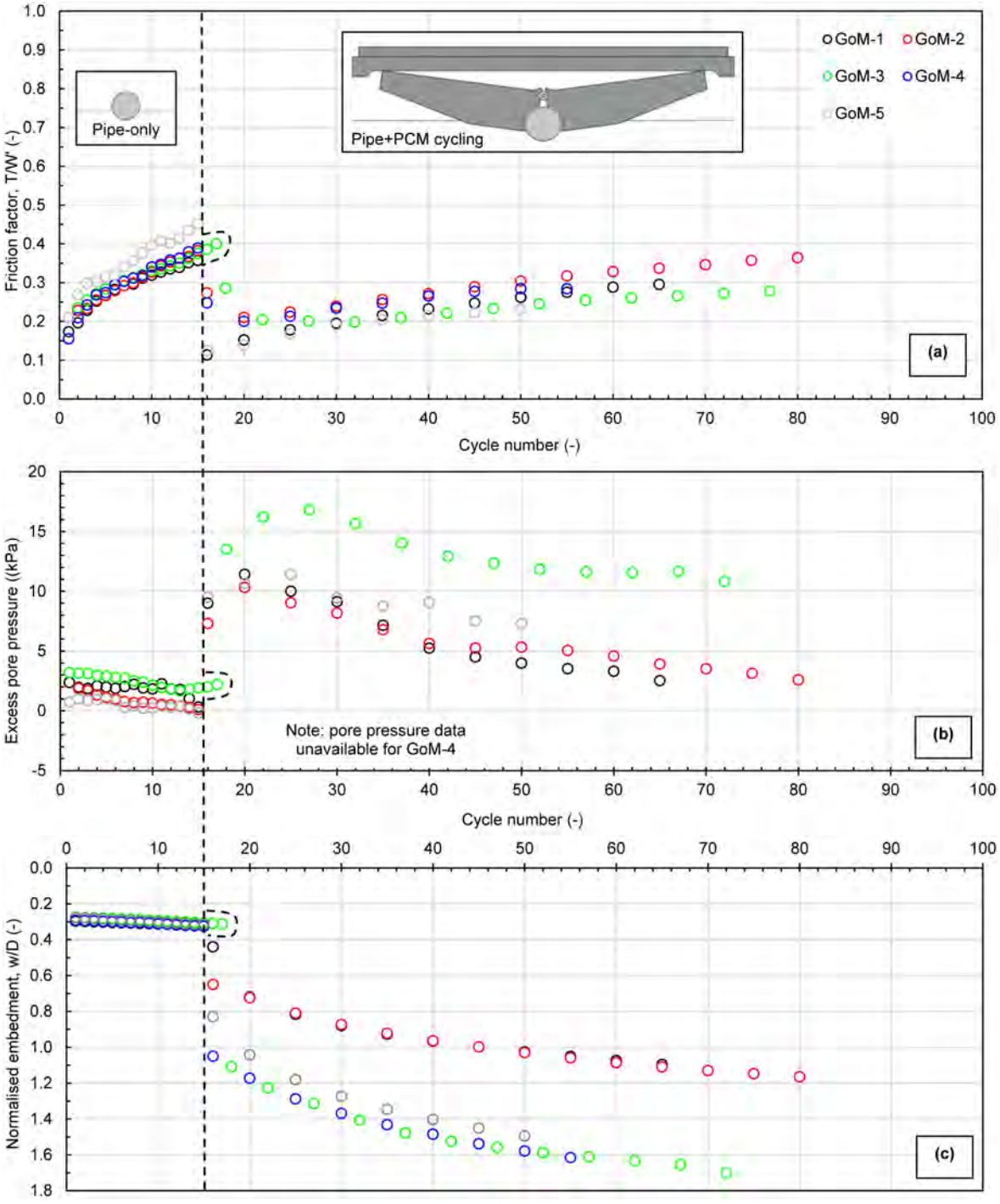

Figure 8—GoM test series cycle-by-cycle results (the step in each test response in the range of cycle 15-17 is the PCM installation)

Observations from the embedment and pore pressure data during the GoM test series are as follows:

6. Pipe embedments increase modestly during the 'pipe-only' cycling, by up to 0.05D. Excess pore pressures trend towards zero over the course of these cycles, confirming that drained conditions are approached.
7. Pipeline embedment increases significantly with PCM placement – typically by about 0.3D for the 50% weight PCM and up to about 0.8D for the 100% weight PCM. Use of the long pipe does not appear to reduce the initial embedment significantly.
8. Excess pore pressures rise sharply with PCM placement, reflecting the rise in total stress. The highest pore pressures correspond to placement of the 100% weight PCM on the short pipe, which is to be expected since the greatest load is spread over the smallest area. Consolidation leads to a reduction in these excess pore pressures, although at a slower rate than during the pipe-only cycles.
9. For the 100% weight PCM tests, the pipe settled to an invert embedment of up to ~ 1.7 diameters (relative to the sample surface) over the course of (forced) cycling. Relative slippage between the PCMs and the pipe was not observed, despite the embedment shifting the reaction with the soil away from the pipe and onto the underside of the PCM (and thus reducing the clamping moment).

Key observation A. The effect of consolidation period between PCM installation and pipe movement

Tests with a longer consolidation period between PCM placement and first movement (1 year vs. 1 week) yielded more than double the peak friction (see Figure 9 – the pink highlighted cycle, $T/W' = 0.35$ vs. 0.14). However, the higher frictions are partially lost with further axial cycling of the pipeline. After a few cycles the difference is reduced to 0.20 vs. 0.15 (the cyan highlighted cycle in Figure 9).

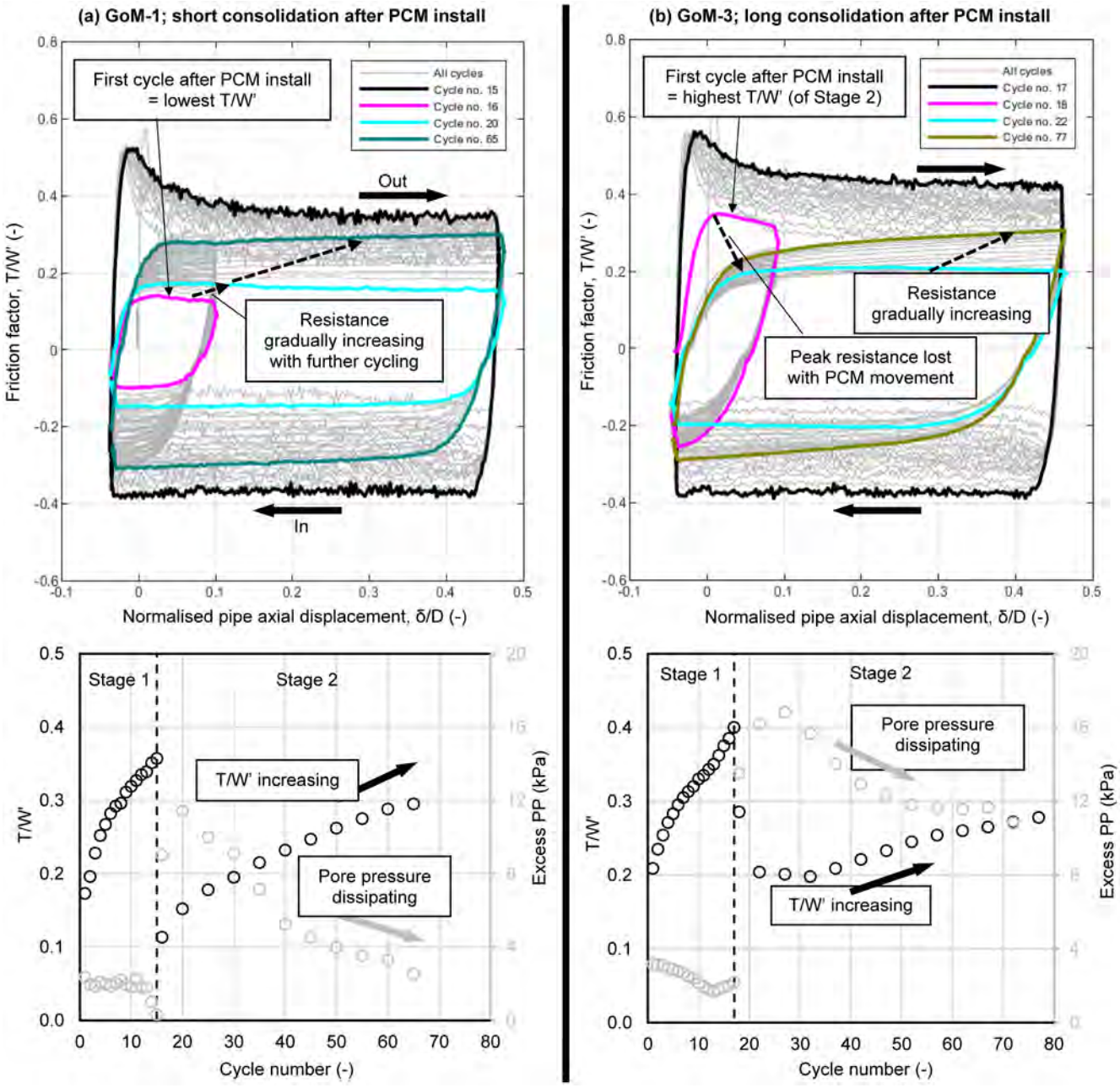

Figure 9—Consolidation effects for 100% weight tests in GoM

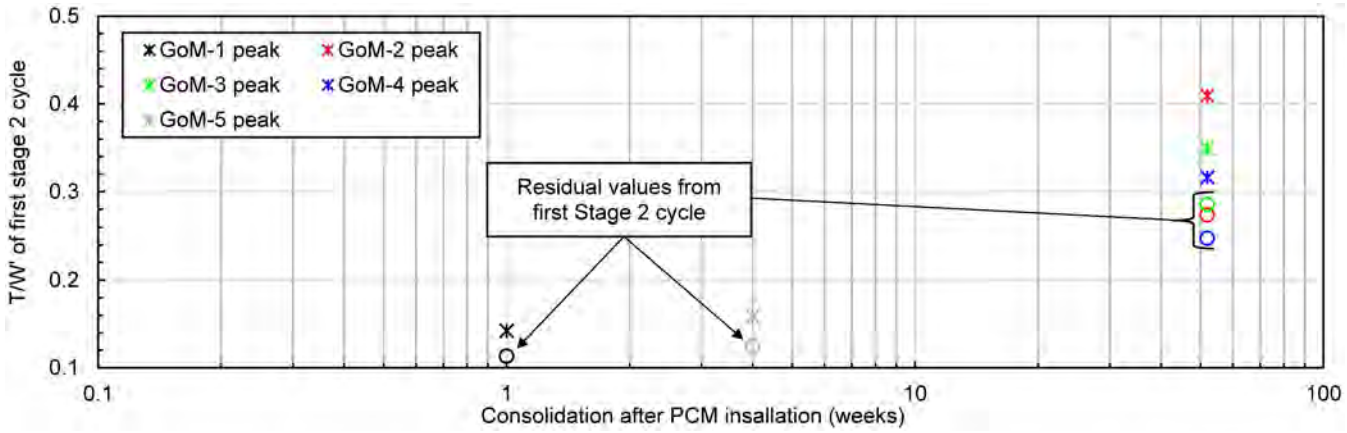

Figure 10—Effect of post-installation consolidation time on next cycle friction (GoM) (asterisks: peak values, circles: residual values)

Throughout the remainder of these two tests, the friction factors progressively increased over time, reaching ~0.3 by the end of each test. Meanwhile, the excess pore pressure continued to fall (see lower plots in Figure 9), but neither the pore pressure or the friction reached stable final drained values.

The influence of the initial consolidation time between PCM installation and first movement is illustrated for all GoM tests in Figure 10. The 'peak' values correspond to the maximum friction factors developed near the beginning of the first Stage 2 outward sweep, while the other residual values are as presented previously (i.e. averages from towards the end of the outward and inward sweeps).

Key observation B: Effect of consolidation period between movements on peak in friction

Notable peaks in the friction response are evident at the start of the outward 'pipe-only' sweeps in all the GoM testing, as annotated for GoM-3 in Figure 11. This outward movement follows a longer pause (representing an operating period) compared to the inward phase (which immediately follows the outward movement, representing a brief shutdown period). This pause during 'operation' allows the pore pressures to dissipate and results in a peak in shear strength followed by strain softening behaviour to a constant ('residual') value.

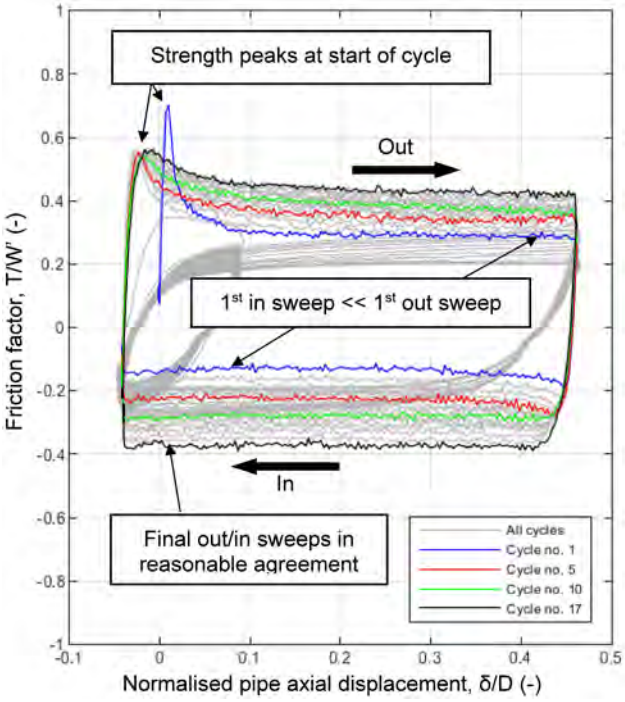

Figure 11—Peak friction factor at beginning of Stage 1 cycles (GoM-3 as example)

A much smaller 'peak' shear strength was observed for the first Stage 2 cycle (with the PCM installed) following long (~ 1 year) consolidation periods. However, apart from this first cycle, no other peaks were observed. This indicates that the 2-week period between Stage 2 cycles was insufficient to allow for noticeable consolidation hardening below the PCM. Furthermore, there were no 'peak' shear strengths for the first Stage 2 cycle of GoM-1 and GoM-5 (featuring the much shorter consolidation times after PCM placement).

Overview of WAf test series observations

The cycle-by-cycle measurements of friction, excess pore pressure at pipe invert and pipe embedment, from all of the WAf tests are summarized in Figure 12. Observations from the friction response are as follows:

1. Before installing the PCM, initial friction factors for the 'pipe-only' test stages are in the range 0.39 - 0.51. This friction increases with axial cycles of the pipe, likely approaching (but not fully reaching) the drained capacity. By cycle 15, friction factors are generally in the range 0.7 – 0.98. Somewhat higher friction values in WAf-2 (1.10) and WAf-5 (1.14) potentially relate to greater wedging effects.
2. After installing the PCM, initial friction factors are generally in the range 0.19 - 0.29 over the first axial cycle (typically cycle #16). As with the 'pipe-only' test stage, the friction gradually increases over the course of each test, with values of 0.45 to 0.67 recorded for cycle 40 (excluding WAf-3 which featured only very small displacement cycles), i.e. typically >100% increase compared to the first cycle after PCM installation. This rise in friction appears to be ongoing at the end of each test, so the steady state friction would be higher than these measured values, and therefore closer to the friction factors measured for the 'pipe-only' stage (as drained conditions are approached).
3. Tests with longer (~ 1 month) consolidation periods following PCM placement yielded somewhat higher peak friction over the very first axial cycle, when compared to tests with a shorter (1 week) consolidation period.
4. Similar initial friction factors for the 50% and 100% weight PCMs are observed after PCM placement.

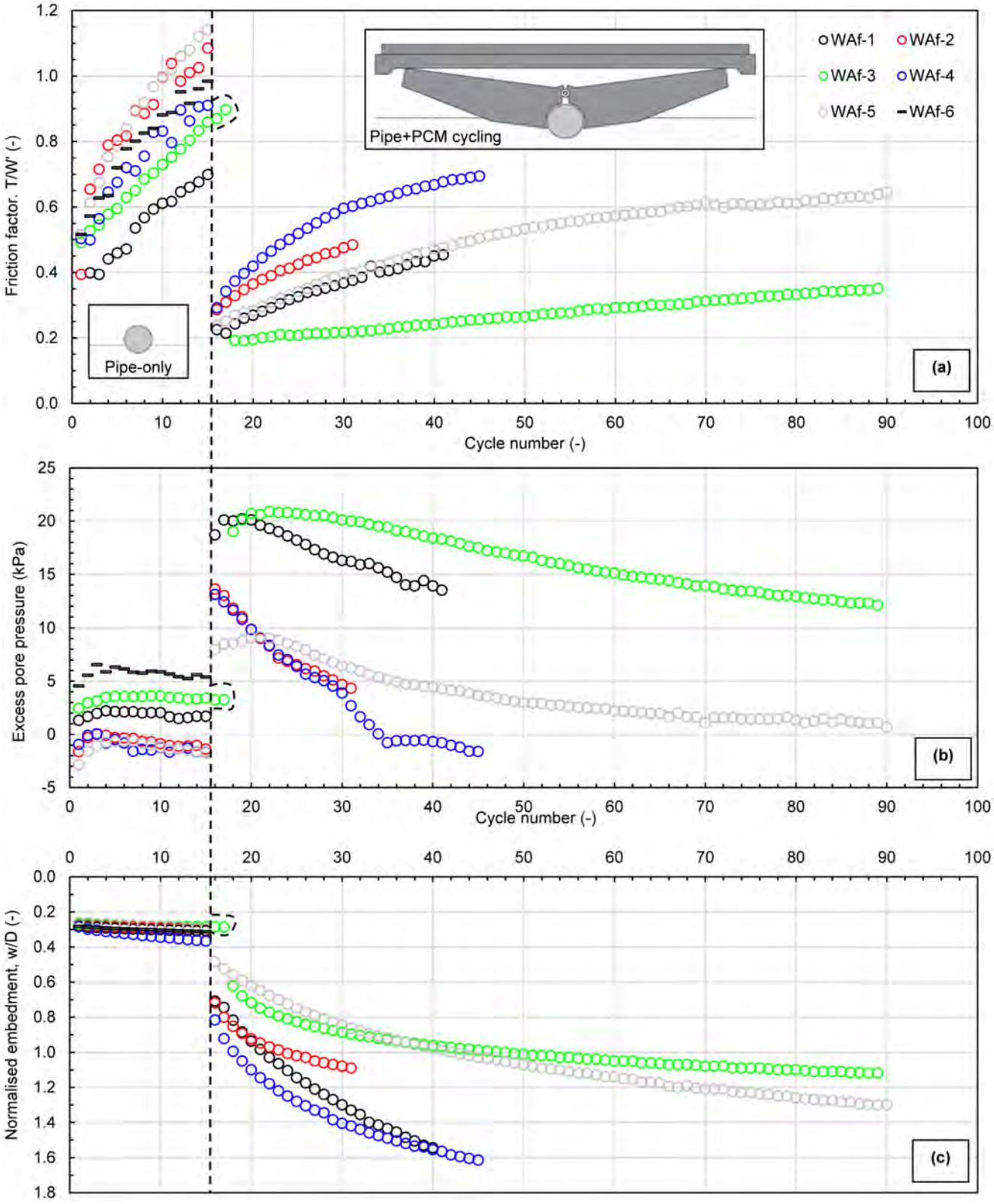

Figure 12—WAf test series cycle-by-cycle results

Observations from the embedment and pore pressure data during the WAf test series are as follows:

5. Pipe embedments increase modestly during the 'pipe-only' cycling, by up to 0.08D. Excess pore pressures trend towards zero over the course of these cycles, confirming that drained conditions are approached.
6. Pipeline embedment increases significantly with PCM placement – by about 0.2D for the 50% weight PCM and up to about 0.45D for the 100% weight PCM.
7. Excess pore pressures rise sharply with PCM placement, reflecting the rise in total stress. The highest pore pressures correspond to placement of the 100% PCM which is to be expected. Consolidation leads to a progressive (and slow) reduction in these excess pore pressures throughout each test.
8. For the 100% weight PCM tests, the pipe settled up to ~ 1.6 diameters (relative to the sample surface) over the course of (forced) cycling. Relative slippage between the PCMs and the pipe was not observed, despite the embedment shifting the reaction with the soil away from the pipe and onto the underside of the PCM (and thus reducing the clamping moment).

Key observation C. The effect of consolidation period between PCM cycles and walking magnitude

Friction factor progression with time for the WAf tests is shown on Figure 13a for Stage 2. As noted previously, longer consolidation periods after PCM placement yielded higher friction factors over the first axial cycle in Stage 2. Figure 13a identifies that the first axial cycle for those longer consolidation tests (WAf-2 and WAf-4) are in good agreement with the T/W' time trends of WAf-1 and WAf-2.

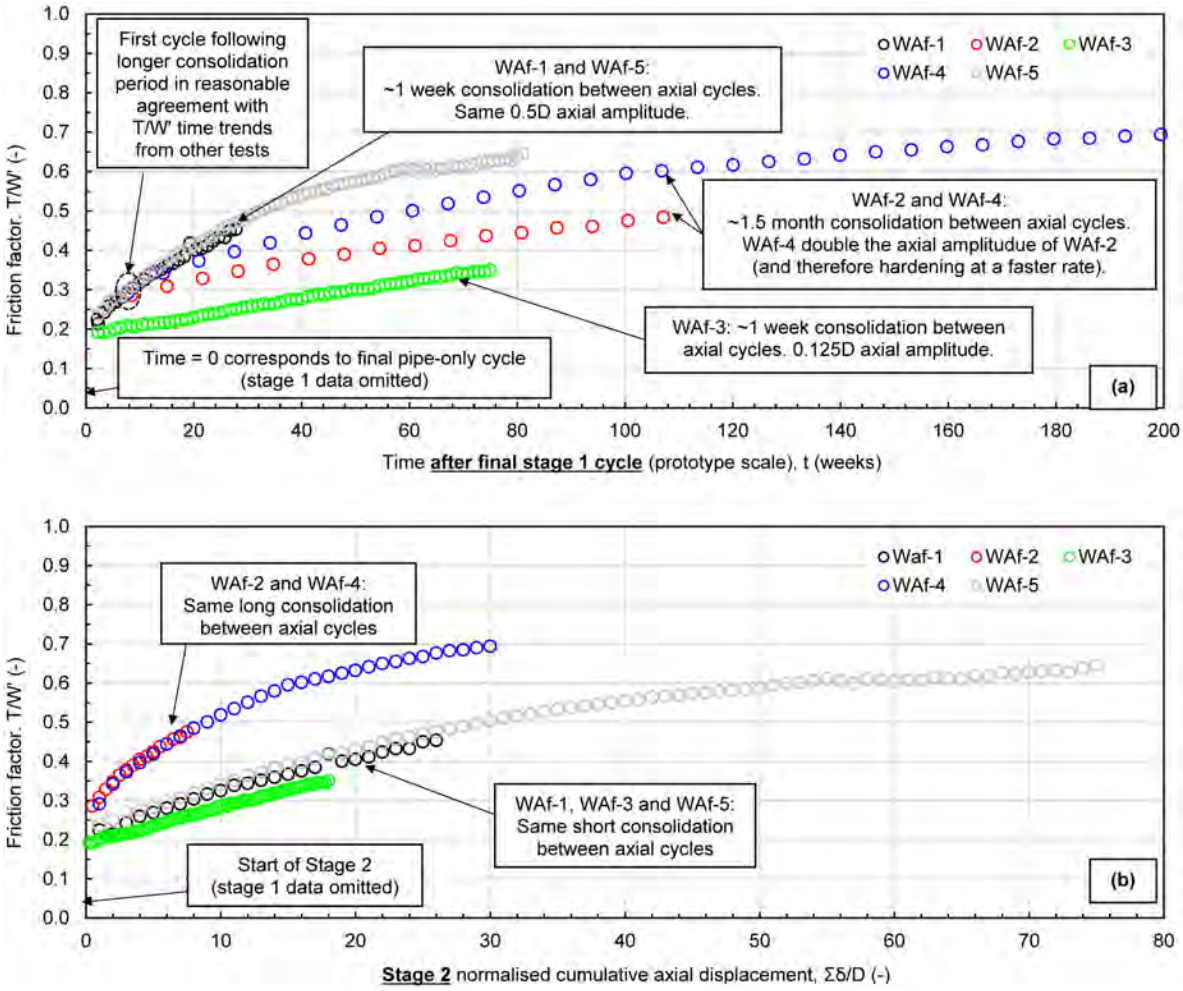

Figure 13—WAf friction factor development for stage 2: (a) with time (b) with cumulative axial displacement

The hardening behaviour for WAf-1 and WAf-5 is similar, despite WAf-5 using 50% weight PCMs, reflecting their equal 1-week consolidation period between cycles and displacement magnitude. With more frequent cycles, the hardening was faster in WAf-1 and WAf-5 than test WAf-4 which featured a longer 1.5 month period between cycles (but the same displacement magnitude). This is because the more frequent movements keep the excess pore pressure 'charged', which creates strength gain through dissipation. With less frequent cycles, once the pore pressure dissipation is complete or has slowed, minimal strength gain occurs until the next cycle. Numerical simulations of similar episodic foundation movements also show this effect (Feng & Gourvenec 2016). Cyclic hardening in WAf-2 was slower than in WAf-4 due to the lower displacement amplitude in WAf-2.

To compare the different cyclic displacement amplitudes in Stage 2 of the WAf test series, Figure 13b compares the friction factor progression with cumulative axial displacement. WAf-1, WAf-3 and WAf-5 featuring the same 1-week consolidation periods between cycles are in good agreement. For a given number of cycles, the highest friction is developed with longer consolidation periods between cycles, indicating in this instance a stronger influence for consolidation on T/W' than for cycling frequency.

Results and observations – silty sand

The cycle-by-cycle measurements of friction, excess pore pressure at pipe invert and pipe embedment, from all of the SS tests are summarized in Figure 14 . Observations from the friction response are as follows:

1. Before installing the PCM, initial friction factors for the 'pipe-only' test stages are generally in the range 0.57 - 0.78. This friction gradually reduces over the first ~10 (pipe-only) cycles before stabilising to factors of about 0.5 - 0.6 (excluding test SS-6).
2. The comparatively lower frictions in SS-6 correspond to overexposure of the pipe before the Stage 1 axial cycling (refer to Table 6 note). This is considered to reflect the release/elimination of wedging effects (discussed later as a key observation).
3. After installing the PCM, initial friction factors generally agree well with those towards the end of Stage 1. The only test not exhibiting good agreement was SS-3 whose friction factor dropped by ~ 15% from the end of Stage 1 to start of Stage 2. This test featured overexposure of the pipe before the Stage 2 axial cycling (refer to Table 7 note) and the friction factor drop is considered to reflect the release/elimination of wedging effects (discussed later as a key observation).
4. Further axial cycling in Stage 2, led to substantial system embedment and corresponding large increases in friction factor. This trend was observed in all tests in the granular material- with high frictions developed over less than 4D of cumulative axial displacement (i.e. 'walking'). The sharp friction increases appear to correspond to the touchdown of the PCM with the sample surface.
5. Following the initial sharp increases over the early Stage 2 cycles, the friction factors plateau with only modest increases over the remainder of each test, clearly shown for up to 100 axial cycles on Figure 14. Overall, friction factors for the full system stabilised 10% to 50% higher than for the pipe alone (to values between 0.62 and 0.83 after 100 cycles).
6. Higher friction factors (of up to about 35%) were observed for the 100% weight PCMs (vs. the 50% weight).
7. SS-1 comprised only large (0.5D) axial displacements and did not feature 'packets' of small/large cycles like all other tests in the silty sand. Interestingly, friction factors in SS-2 appear to reduce with cycles, but from an initially high T/W' jump (of around 40%) after PCM placement and completion of the first set of small amplitude cycles. This is thought to reflect embedment during the small cycles, with the resistance trending towards a value broadly comparable to Test 1.

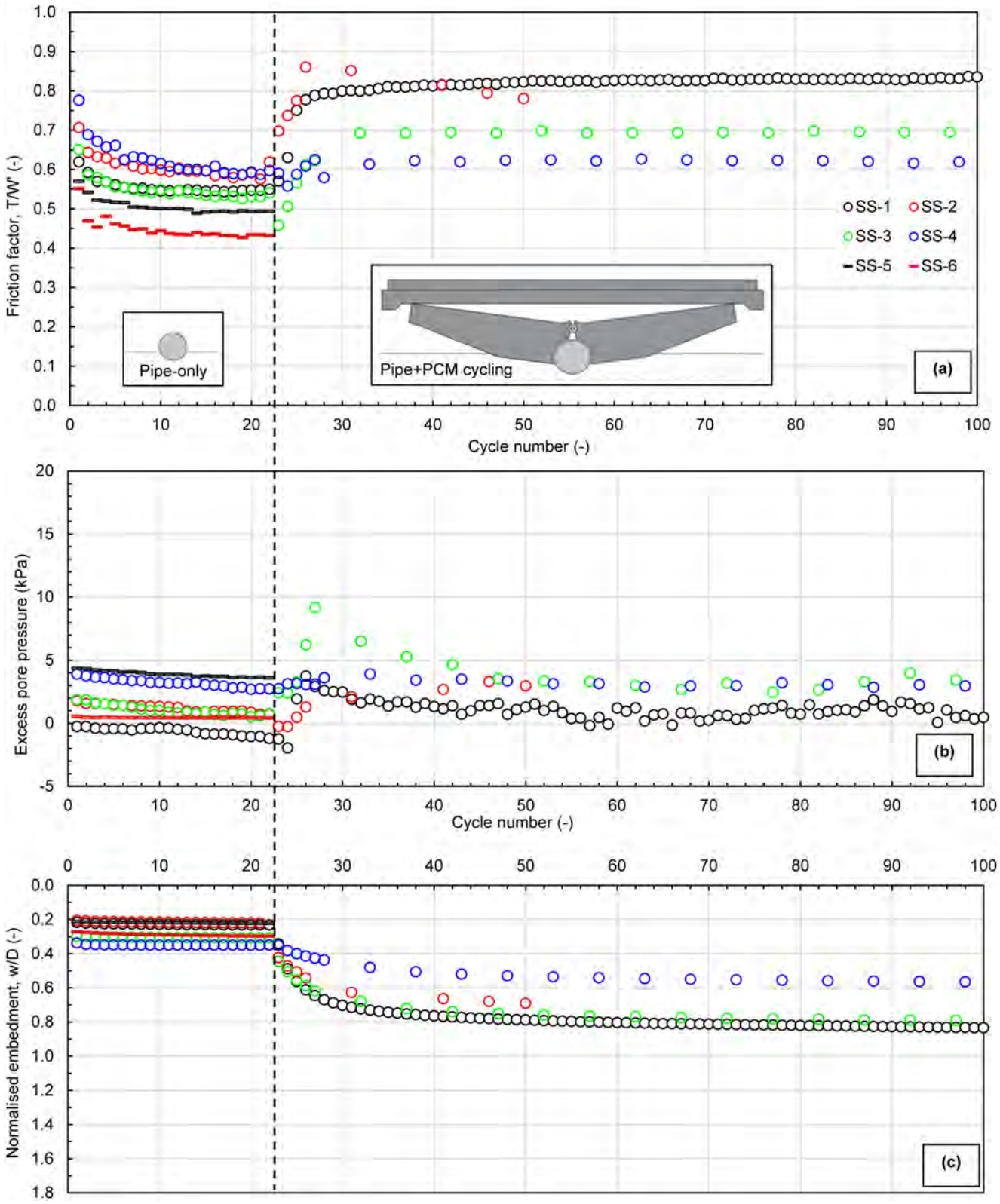

Figure 14—SS test series cycle-by-cycle results

Observations from the embedment and pore pressure data during the SS test series are as follows:

8. Ongoing embedment was negligible during pipe-only axial cycling and limited to about 0.01D. Excess pore pressures remained close to zero over the course of these cycles; a result of the more drained material.

9. Pipe embedment increased significantly (relative to overall test embedment) during the very early axial cycles following PCM placement before plateauing.
10. Excess pore pressures remained relatively low with PCM placement, reflecting the more drained material. The exception to this was test SS-3 which exhibited an increase of ~8 kPa in pore pressure during the very early axial cycles following PCM placement. However, this is expected to be artificial and potentially a result of the soil scraping (overexposure) techniques interfering with the pore pressure transducer located at the pipe invert.
11. For the 100% weight PCM tests, the pipe settled up to ~0.85 diameters (relative to the sample surface) over the course of (forced) cycling. Relative slippage between the PCMs and the pipe was not observed.

Key observation D: Substantial embedment and increased friction with early PCM cycling

Frictions in the silty sand (SS) tests did not progressively rise with pore pressure dissipation/consolidation as observed in the clays. Instead, excess pore pressures remained reasonably low throughout the tests- even during (and directly after) placement of the PCM - because of the more drained conditions.

As shown in Figure 14, sharp friction and system embedment increases took place over the early Stage 2 cycles. This is clearly annotated for an individual test (SS-3) in Figure 15. The first cycle following PCM placement in SS-3 (no. 23) yielded the lowest friction factor across the test. Note: this friction factor drop was not recorded in other tests and is due to overexposure of the pipe following Stage 1 in this specific test. Following this sharp increase event, the friction factors and system embedment plateau with only modest increases over the remainder of the test.

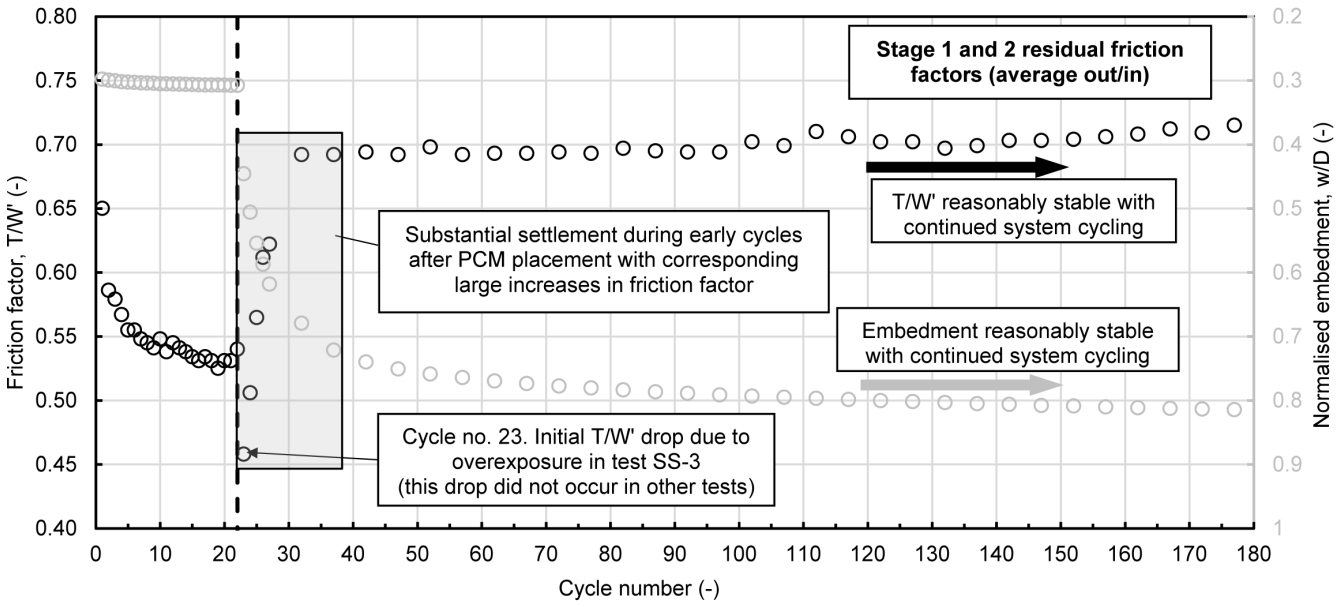

Figure 15—Substantial embedment and increased friction with early PCM cycling (SS-3 as example)

Key observation E: Wedging effects (following from key observation D)

As cited throughout this paper, 'wedging' effects are understood to influence the system friction factors. Wedging simply refers to the enhanced friction caused by non-vertical normal stresses acting along the pipe-seabed interface as depicted in Figure 16. These non-vertical normal stresses lead to a normal contact force with the seabed that exceeds the weight. As a result, the seabed sliding resistance becomes greater than the weight multiplied by the interface friction coefficient (which is the case for a planar contact). The circular shape of a pipe leads to non-vertical pipe-seabed contact forces, which increase with pipe embedment. The resulting wedging effect has been accounted for in other studies of axial pipe-soil friction, following the

solution of White & Randolph (2007), which is used as standard in pipe-soil friction assessments, following DNV RP F114 (2019).

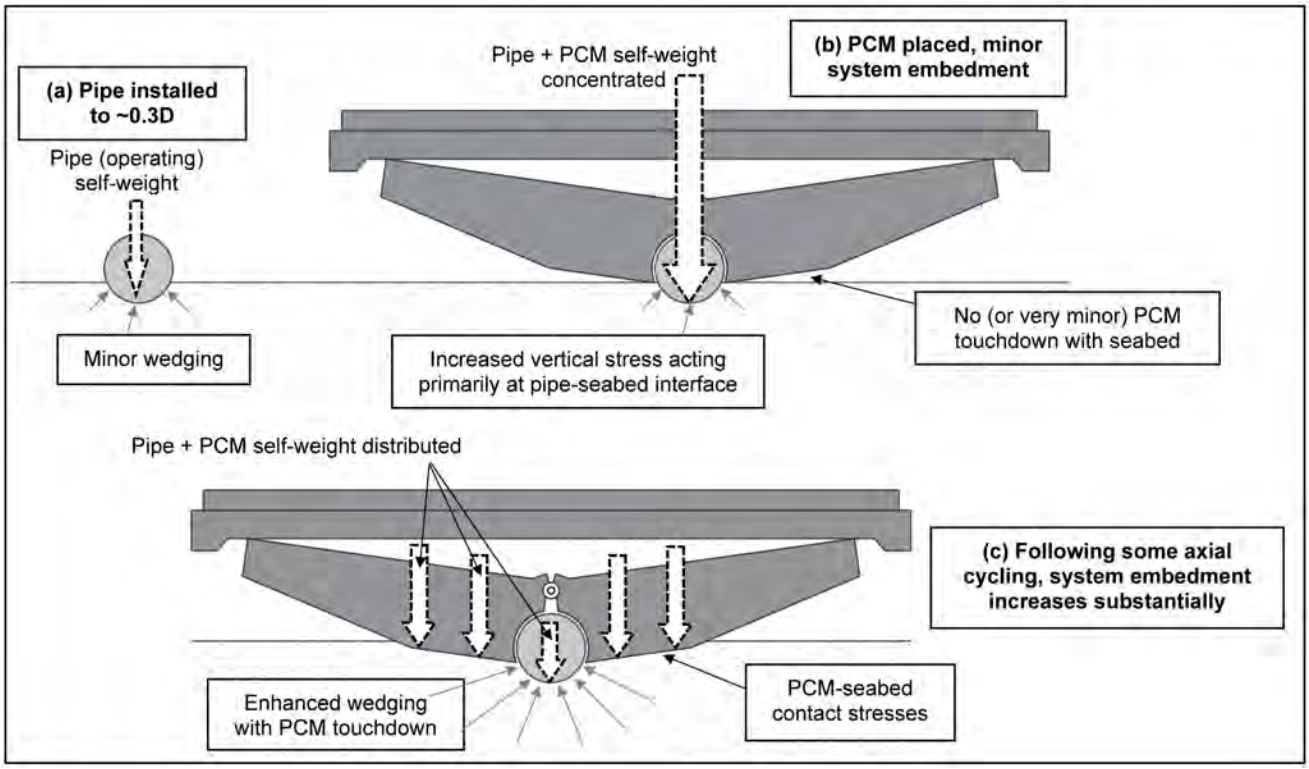

Figure 16—Wedging (and 'enhanced' wedging) schematic in granular material

Stage 1 (pipe only) wedging effects in silty sand. As seen in Figure 17a, differences between the Stage 1 friction factors were observed across the silty sand tests SS-1 to SS-5 (i.e. T/W' not always in good agreement). Although the same test conditions were adopted (pipe operating weight, axial cycling displacements etc.), with a constant target of 0.3D initial embedment – careful review of the processed pore pressure data (measured at the pipe invert) revealed that there were slight variations in the actual embedment. To explore this effect further, an additional pipe-only 'control' test was completed (SS-6), in which the pipe was overexposed before the Stage 1 axial cycling (refer to Table 6 note). Notably, this test exhibited comparatively lower friction factors reflecting a release/elimination of wedging effects.

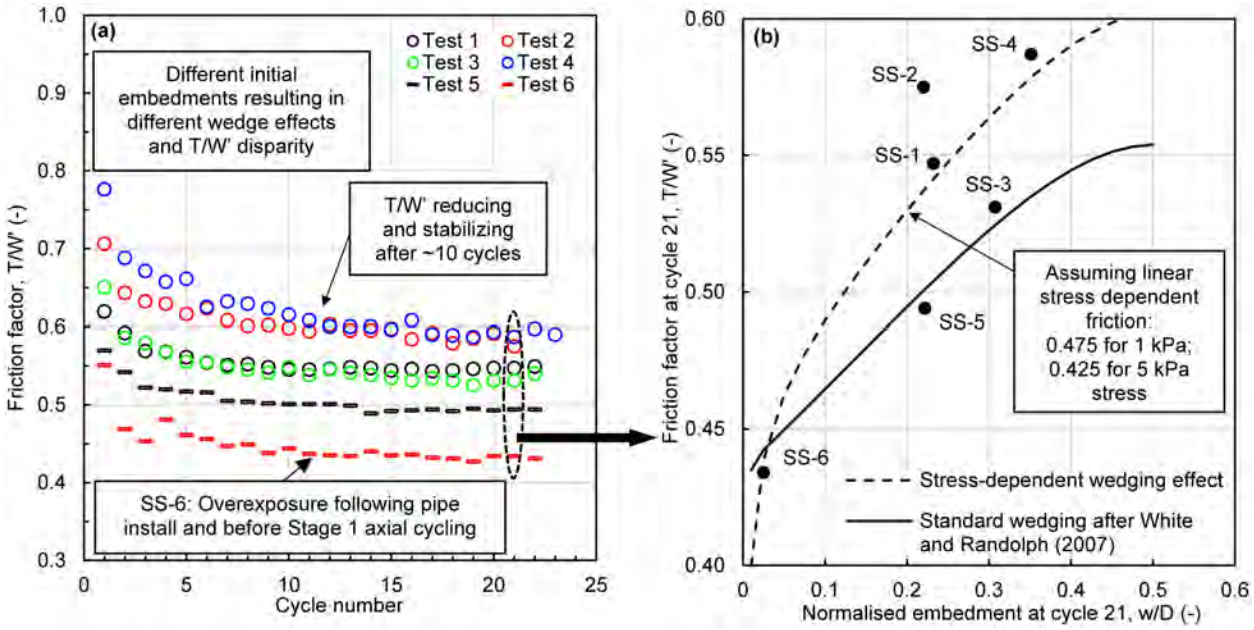

Figure 17—Wedging effect for Stage 1 (pipe-only)

Figure 17b shows relationships between pipe embedment and the 'pipe-only' friction factors based on two approaches. Firstly, the conventional White & Randolph (2007) wedging effect, which allows for the enhanced normal force due to inclined stresses around the pipe periphery. Secondly, an extended version of this approach, in which the interface friction factor reduces with stress level, consistent with the interface test results. This extension creates a stronger overall influence of embedment on friction factor, because at low embedments the mean contact stress is higher, so a lower friction factor applies. The extended stress-dependent wedging model fits the test results better than the standard wedging solution.

Furthermore, it is expected that the gradual reduction in friction factor over the first ~10 (pipe-only) cycles corresponds to a reduction in normal contact force due to a wedging effect release. The vertical load would then concentrate towards the pipe invert and tend to raise the stress level at the pipe-soil interface, thus reducing the interface friction angle (i.e. effect of stress level on soil friction angle).

Stage 2 (pipe + PCM) wedging effects in silty sand. For the silty sand tests, the initial Stage 2 friction factors mostly agree with those towards the end of Stage 1 as previously identified in Figure 14. High system settlements and frictions were developed over less than 4D of cumulative axial displacement (i.e. 'walking') in Stage 2 as shown in Figure 18. The sharp friction increases appear to correspond to PCM touchdown on the sample surface. The PCM has non-vertical surfaces, and there is also interaction between the pipe and PCM which may enhance the wedging effect due to the PCM creating a surcharge load adjacent the pipe (Figure 16). The wedging enhancement is now understood to result from the vertical load of the PCM being redistributed around the pipe as the system embeds and the base of the PCM contacts the mudline.

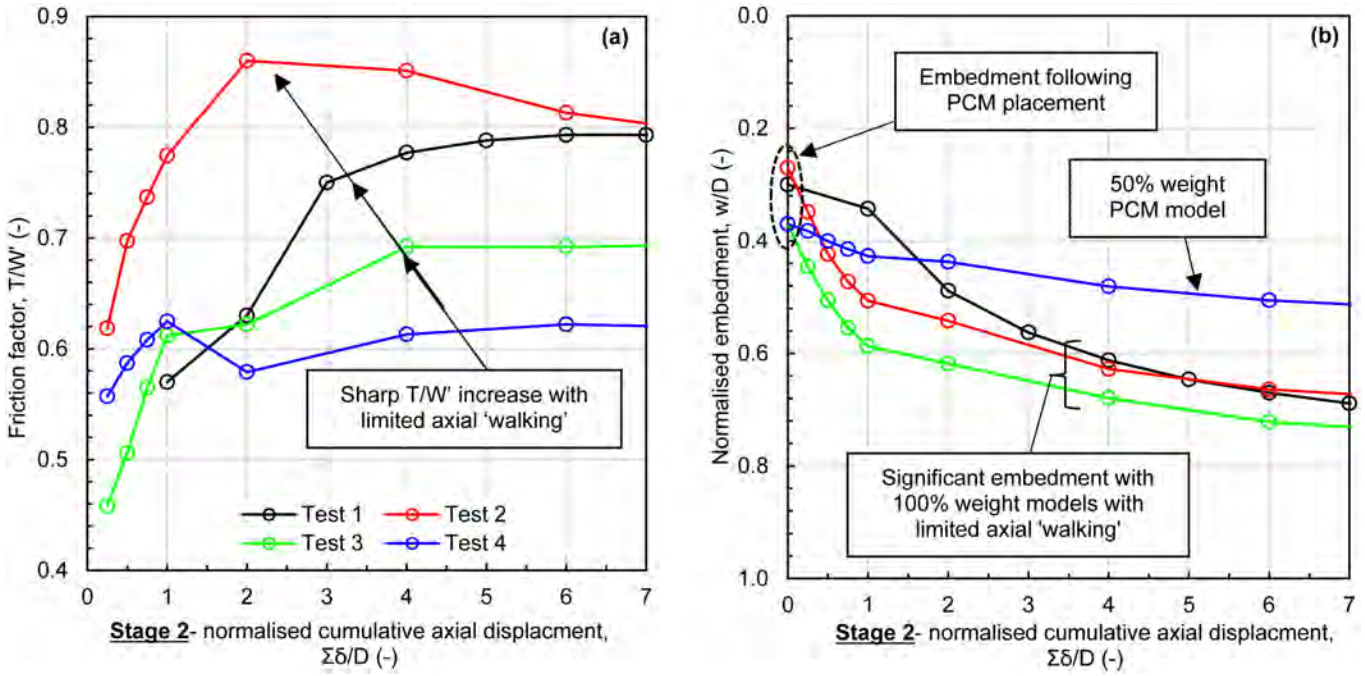

Figure 18—Enhanced wedging linked with significant system embedment in Stage 2

The concept of an enhanced wedging mechanism is further reinforced by reconsidering the over-exposed pipe in test SS-3 and its notably lower friction factor as mentioned previously (from end of Stage 1 vs start of Stage 2). The soil scraping/overexposure results in the release/elimination of wedging effects and thus the corresponding lower friction factors in Stage 2. Additionally, SS-4 (featuring the 50% weight PCM model) yielded the smallest increases in friction factor (relative to Stage 1) showing that the enhanced wedging effect is dependent upon the magnitude of vertical stress applied by the PCM.

Key observation F: Effect of 'pause' period between movements on peak in friction in silty sand

Unlike the clays, no notable peaks in the friction response were evident at the start of the outward 'pipe-only' sweeps as shown in Figure 19a. This indicates negligible excess pore pressure dissipation (and corresponding friction gain) occurs in the more granular (drained) material. The data also indicate the nominal stress applied by the pipe-only (~ 1.4 kPa) does not lead to any noticeable volumetric strain upon shearing. Interestingly, small friction factor peaks appear towards the end of both the outward and inward sweeps during the pipe-only cycling. This was observed in the majority of the silty sand tests and is believed to be due to berm build-up/interference.

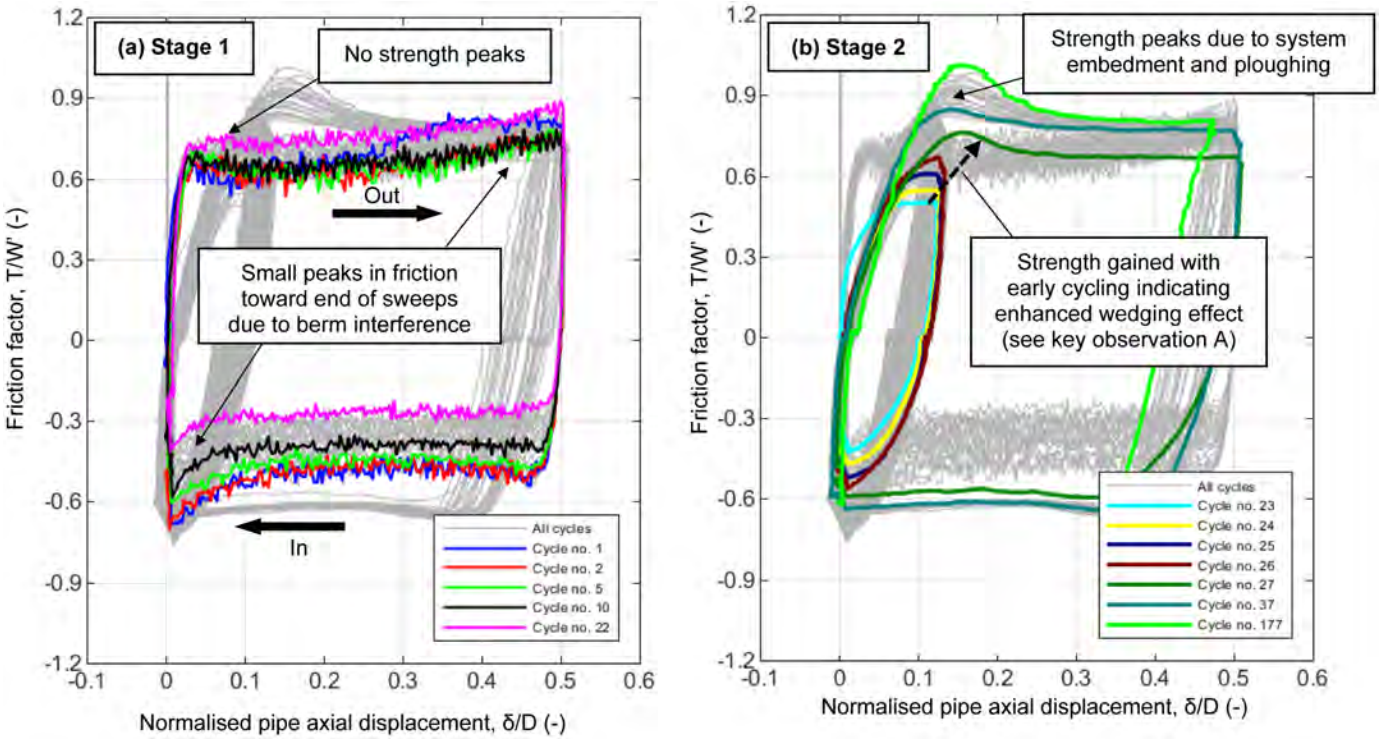

Figure 19—No peak friction factor due to excess pore pressure dissipation (SS-3 as example)

Furthermore, clear friction factor peaks are observed towards the beginning of the Stage 2 cycles for SS-3 as on Figure 19b. This observation was less distinguishable in several of the other of the silty sand tests and is believed to be due to system embedment and ploughing (i.e. not applicable to field conditions).

Reflecting on PCM performance

Overview of base friction performance vs ISB tests

An overview of pipe and PCM friction responses from the three centrifuge test series is given in Figure 20. The first and final cycle friction factors (for example: data points for cycle 1, 15, 16 and 65 for GoM-1 on Figure 7) are illustrated for a base case test in each of the different offshore soils (WAf-1, GoM-3 and SS-1).

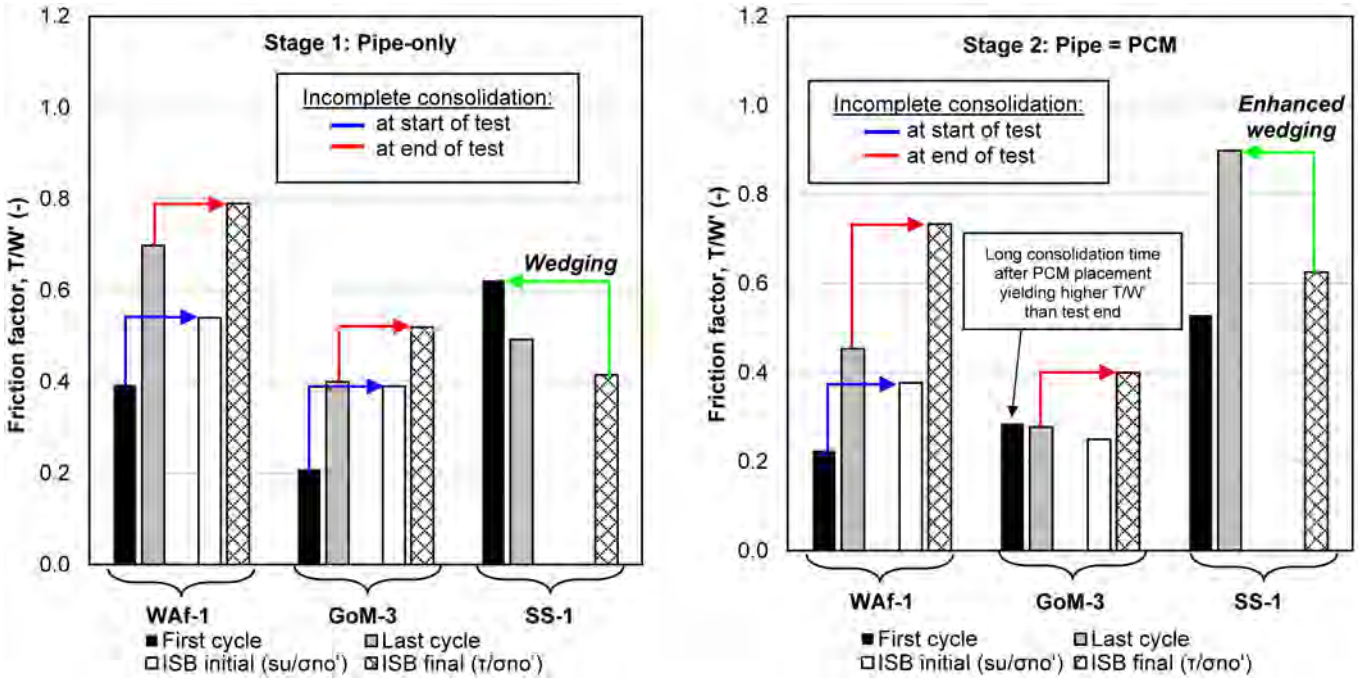

Figure 20—Overview of pipe and PCM performance (pipe/PCM frictions: black and grey; ISB frictions: white and hatched)

Before installing the PCM, initial friction factors for the pipe-only are generally around 0.4 or 0.2 for the West Africa and GoM clays respectively. These frictions increase with continued axial cycles, approaching the drained capacity. In contrast, much higher friction factors of around 0.6 to 0.7 were initially observed in the silty sand which tended to slightly decrease during early cycling. The pipe-only T/W′ values in the clays are slightly lower than from the ISBs, which is attributed to incomplete consolidation under the pipe weight. In contrast, the pipe-only T/W' in the silty sand is greater than the drained ISB friction, suggesting there is a 'wedging' mechanism which is less (or not) evident in the clays.

The friction gains developed during the pipe-only cycling in the both clays are 'lost' upon PCM placement, due to the additional weight of the PCM being initially carried by excess pore pressure. For the WAf clay, the initial Stage 2 friction factors were below those observed at the start of pipe-only cycling. The friction gradually increased with further cycling, but at a slower rate than that of the pipe-only. This reflects the longer dissipation times required for the larger foundation area (and greater drainage lengths). The GoM-3 test performed better (in terms of friction) with the first cycle due to a long consolidation time incorporated following PCM placement. However, as previously outlined this quickly dropped lower once Stage 2 cycling was initiated. In fact, GoM-3 did not recover its initial Stage 2 friction by the test end.

For the silty sand, the friction factor did not drop upon PCM placement. Instead, initial Stage 2 cycles had comparable friction to Stage 1 – indicating no major excess pore pressure generation. Interestingly, T/W' then quickly increased (and stabilized) by up to ~ 50% with only a few more axial cycles. This trend was not reflected in the ISB tests and is thought to be due to a redistribution of the vertical load around the pipe, activating the enhanced 'wedging' effect discussed earlier.

Overall embedment observations

Due to differences in cycle regime, it is convenient to plot embedment against cumulative axial displacement. This is presented in Figure 21, where good agreement is evident for tests performed with the same PCM weight – confirming that embedment is a function of axial displacement. Some review comments comparing the clay vs silty sand are offered below.

- In clay, pipe embedment increased during the pipe-only cycling – although this was modest (limited to about 5% of the pipe diameter). Small excess pore pressures (of only a few kPa) are seen to dissipate during cycling, trending towards zero as expected. For the silty sand, negligible pipe embedment was observed during Stage 1, typically less than 1% of the pipe diameter and with negligible excess pore pressures generated.
- For both the GoM and WAf soils, the system settled by about 1D once the PCMs (clamp + log mattress) were installed, with correspondingly high excess pore pressures being generated (up to 20 kPa under the 100% weight models). Settlement of up to 10% of the pipe diameter was observed during consolidation, prior to further axial cycling. For the silty sand, embedment less than 0.1D was observed when placing the PCM (even for a test where sand had been excavated either side of the pipe), with negligible excess pore pressures and no significant consolidation settlement.
- During axial cycling in the clay soils, the pipe embedded by as much as 1.5 pipe diameters (for the 100% PCM weight case) relative to the original seabed level, following 10D of cumulative axial walking in Stage 2. Consolidation resulted in a progressive reduction in excess pore pressure throughout cycling, consistent with an increasing friction factor. Overall embedments in the silty sand were far lower, with the greatest settlements observed during the first few small (0.125D amplitude) axial cycles before plateauing. Maximum system embedments were around half those observed in the clay tests.

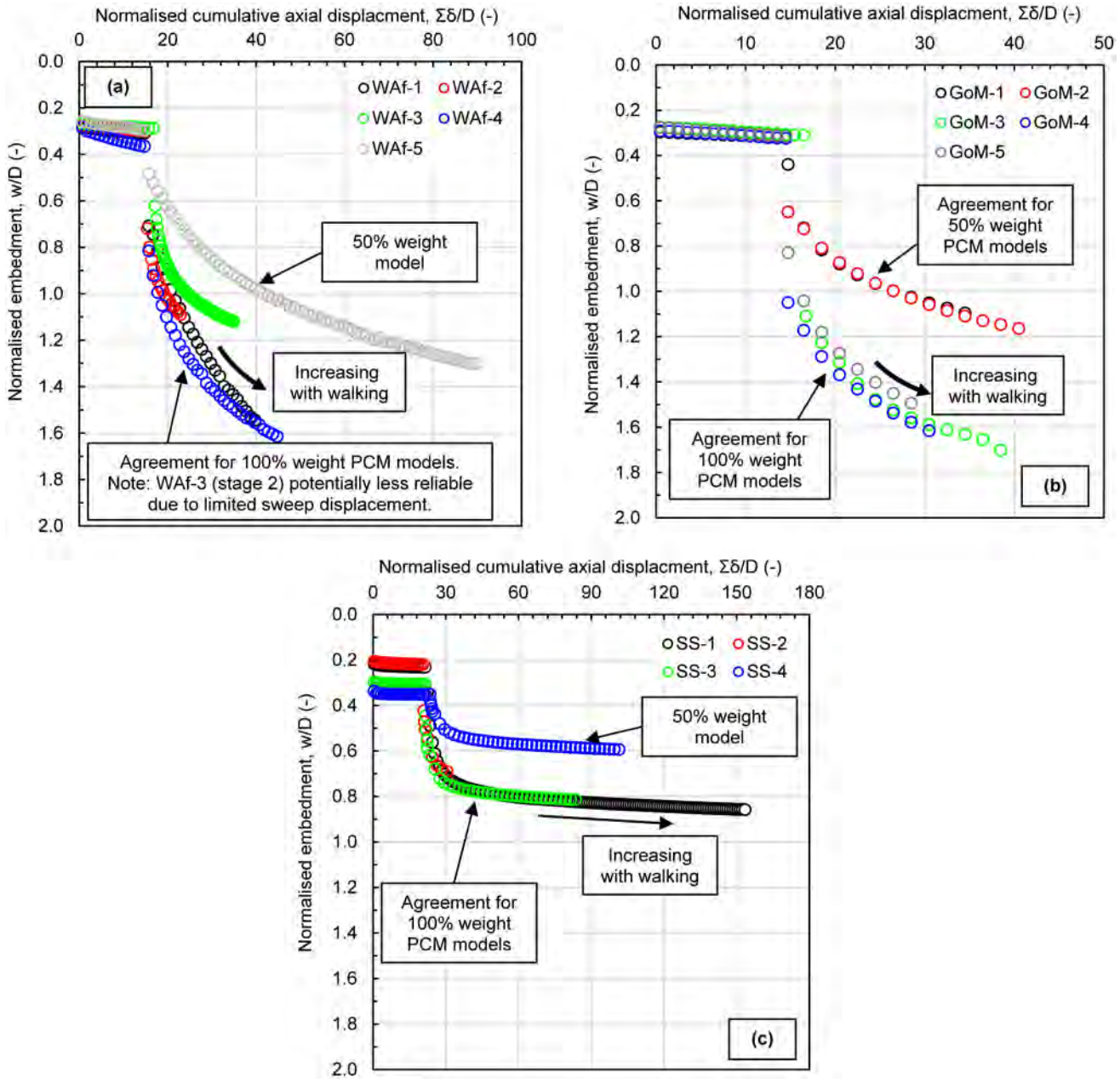

Figure 21—Embedment with axial displacement: (a) West Africa clay (WAf); (b) Gulf of Mexico clay (GoM); (c) carbonate silty sand (SS)

Ongoing work

Although pipe overexposure tests, representing the effect of erosion of sediment around the pipe, are reported in this paper, the influence of scouring is outside the scope of the current study. Wedging, together with any enhancement upon PCM touchdown with the seabed, may be affected by scouring in offshore granular sediment, in mobile bed conditions. A more comprehensive investigation on scouring around PCMs is in progress, with physical modelling being carried out in a closed-loop flume at the University of Western Australia's O-Tube facilities.

The centrifuge results reported in this paper are presently being used to develop updated design guidelines encompassing an analysis framework for axial pipe-soil resistance and PCM-soil sliding resistance. The framework is expected to emphasize the pertinence of intent based scopes for geotechnical surveys and

laboratory testing. The analysis framework along with findings from the scouring investigation will be reported in due course.

Concluding remarks

A comprehensive centrifuge modelling program has provided a wide range of data demonstrating the performance and behavior of pipe clamping mattresses (PCMs) in different soil types. PCMs offer an innovative solution to add anchoring force to a pipeline at any location, without the need for pre-installed lugs or connection points. PCMs are attached to the pipe via a clamping action created by the arrangement of a log mattress resting on a hinged clamp unit. PCMs can be installed at any stage during the operating life of a pipeline, allowing a 'wait-and-see' approach to be used to mitigate the potential for thermally-induced pipeline walking. They are designed to remain fully clamped to the pipe and continue to contribute to anchoring resistance even if the pipe embeds deeper into the seabed.

The following conclusions have emerged from this study:

- Centrifuge modelling, using advanced programmable actuation, allows the full sequence of pipeline operation, PCM installation, and subsequent pipe-PCM behavior, to be realistically modelled. This process reveals the whole-life changes in soil strength and seabed friction due to pipe installation and operation, PCM installation and subsequent pipe-PCM behavior. Changes in friction occur over a period extending to several times the duration of a single dissipation cycle, which corresponds to months or years at field scale in clay. The accelerated consolidation in the centrifuge allows this long term whole-life behavior to be faithfully captured in a test with 1-2 days of continuous spinning.
- On clay soils, the pipe-seabed and PCM-pipe-seabed friction followed trends consistent with axial pipe-soil interaction theory:
    - On initial placement of the pipe or PCM, the applied weight is primarily supported by excess pore pressure, with low effective stress at the seabed interface.
    - After full dissipation of the weight-induced excess pore pressure, the pipe-seabed and PCM-seabed friction is similar to interface strengths from interface shear box tests.
    - During cycles of axial movement interspersed with pause periods, further excess pore pressure is generated and dissipated, leading to a rise in seabed friction towards the drained limit. This 'consolidation hardening' process is already recognized in pipe-seabed friction design methods, and is shown to also apply to pipe/PCM-seabed friction.
    - It is therefore possible to estimate the PCM-seabed friction based on ISB test results. However, the centrifuge tests showed that for realistic intervals between PCM installation and pipeline operation, and between shutdown cycles, full pore pressure dissipation may not occur. In this case, the seabed friction is lower for a period, due to the continued presence of excess pore pressure. A longer period between PCM installation and the first pipeline movement, and a longer period between subsequent pipeline movements, both led to higher seabed friction, reflecting the greater degree of consolidation.
    - Calculations of consolidation rate and measurements of consolidation properties are therefore important to consider in PCM design. The ISB measurements of drained interface friction used to assess pipeline axial resistance may overestimate the friction available on the larger PCM units, for which drainage takes longer. It may be worthwhile exploring any potential opportunities to accelerate consolidation below the PCM, such as the provision for additional drainage holes at the clamp base.
    - Ultimately, the PCM-seabed resistance approaches the drained friction, which provides an estimate of the long-term anchoring force that can ultimately be provided by PCMs.

- On silty sand, the same framework applies, but with consolidation occurring at a higher rate:
  - The seabed friction on the pipe or pipe-PCM system was generally equal or greater than the drained friction measured in ISB tests, reflecting full consolidation between each loading step or shutdown cycle.
  - The seabed resistance for the pipe alone showed an apparent enhanced wedging effect. This is attributed to a stress-dependent interface friction angle: at higher embedment the lower average pipe-seabed contact stress contributes to a higher pipeline axial friction, in addition to the conventional wedging effect caused by the inclined contact forces.
  - The seabed friction from the combined pipe and PCM unit was also greater than the drained interface strength measured in shear box tests. This is attributed to an enhanced wedging effect caused by the surcharge load applied by the PCM adjacent to the pipe.
- On all soils, the PCM remained fully attached to the pipe throughout the testing sequence, despite some vertical settlement of the combined system, which could reduce the leverage within the clamp. In the clays, the final embedment of the pipe often exceeded 1.5 diameters, and in the silty sand it typically reached about half that over a similar amount of cumulative 'walking' displacement.

Overall, the centrifuge modelling demonstrates that the PCM offers a highly efficient pipeline anchoring method on different soil types. Rock berms are one of the primary alternative solutions, and were indeed the initial choice for the project where PCMs were first used. Anchoring system efficiency can be defined as the ratio of the anchoring force provided per unit submerged weight of material placed on the seabed. By this measure, rock berms typically provide an efficiency of 10-20%. In contrast, this PCM centrifuge test program reveals long term efficiencies in the range 50-100%, depending on soil type. PCMs are also quick to install using a relatively small offshore installation spread and can be fabricated from conventional (or fibre-reinforced) concrete, so can generally be produced local to the project.

This combination of benefits means that the innovative PCM technology offers a significant cost and schedule improvement to projects seeking to mitigate pipeline walking, as well as environmental benefits from efficient and local material use.

Acknowledgements

The centrifuge testing described in this paper was (independently) funded by three Operators. Shell funding was provided via the Shell Chair in Offshore Engineering at The University of Western Australia, and it is further acknowledged that the PCM concept is subject to a patent application held by Shell. Woodside funding was provided by Woodside Energy Ltd, as operator of the North West Shelf Project Joint Venture, involving BHP Billiton Petroleum (North West Shelf) Pty Ltd, bp Developments Australia Pty Ltd, Chevron Australia Pty Ltd, Japan Australia LNG (MIMI) Pty Ltd, Woodside Energy Ltd and Shell Australia Pty Ltd. Funding from bp was provided under subcontract to Subcon. The authors also gratefully acknowledge technical support during from Andy Hill (bp) and Crondall Energy during planning, execution and review of relevant test campaigns.

Professor Phil Watson leads the Shell Chair in Offshore Engineering research team at The University of Western Australia, which is sponsored by Shell Australia. The UWA authors thank the NGCF team for their support to this test campaign.

References

Bruton, D. (2017). Pipeline Technology-Expansion and Global Buckling. *Chapter in Encyclopedia of Marine & Offshore Engineering, Wiley*. DOI: 10.1002/9781118476406.emoe559

Bruton, D., Sinclair, F. and Carr, M. (2010). Lessons Learned From Observing Walking of Pipelines with Lateral Buckles, Including New Driving Mechanisms and Updated Analysis Models. Offshore Technology Conference, Houston Texas, USA, 3 -6 May 2010, Paper No. OTC 20750.

Carneiro, D., Borges Rodriguez, A., Klinkvort, R. T., Worren, A. and Banimahd, M. (2017). Active Pressure of Rock Berms on Pipelines. Proc. of the 8th Int. Conf, on Offshore Site Investigation and Geotechnics (OSIG) 2017, 12-14 Sept. 2017 London.

Carr, M., Sinclair, F., and Bruton, D. (2006). Pipeline Walking-Understanding the Field Layout Challenges, and Analytical Solutions Developed for the Safebuck JIP, Offshore Technology Conference, Houston Texas, USA, 1-4 May 2006, Paper No. OTC 17945.

DNV (2019). Pipe-soil interaction for submarine pipelines. *Recommended Practice RP F-114*.

Feng, X. and Gourvenec, S.M. (2016). Modelling sliding resistance of tolerably mobile subsea mudmats. *Geotechnique* **66**:6, 490–499.

Frankenmolen, S., Ang, S.-Y., Peek, R., Carr, M., MacRae, I., White, D., and Rimmer, J. (2017). Pipe-Clamping Mattress to Stop Flowline Walking. Offshore Technology Conference. Houstan, Texas, USA, 1-4 May doi:10.4043/27815-MS.

Gaudin, C., O'Loughlin, C., and Breen, J. (2018). A new 240 g-tonne geotechnical centrifuge at the University of Western Australia. In Proceedings of the 9th International Conference on Physical Modelling in Geotechnics (ICPMG 2018) (pp. 501–506). CRC Press.

O'Beirne, C., O'Loughlin, C., Watson, P., White, D.J., Ang, S.-Y. and Frankenmolen, S. (2020). On the Behaviour of Pipe-Clamping Mattresses to Arrest Pipeline Walking. *International Symposium on Frontiers in Offshore Geotechnics (ISFOG 2020)*. Article #3575, Publication #1069.

O'Beirne, C., Watson, P., O'Loughlin, C., Banimahd, M. and Kuo, M. (2021). On the behaviour of rock berms to arrest axial walking of offshore pipelines. *International Conference on Soil Mechanics and Geotechnical Engineering (ICSMGE 2021)*. Accepted for publication.

Perinet, D. and Frazer, I. (2006). Mitigation methods for deepwater pipeline instability induced by pressure and temperature variations. Proc. of 2006 Offshore Technology Conference, Houston, Texas, OTC Paper 17815.

Rodriguez, A. B., Klinkvort, R. T., and Worren, A. (2018). Axial Rock Berm-Pipeline-Seabed Interactions. Offshore Technology Conference, 20-23 March, Kuala Lumpur.

Smith, V.B. and White, D.J. (2014). Volumetric hardening in pipe-soil interaction. Proc. Offshore Technology Conference, Asia. Kuala Lumpur. Paper OTC-24856-MS.

White, D.J. and Bransby, M.F. (2018). Pipeline-seabed Interaction. *Chapter in Encyclopedia of Marine & Offshore Engineering, Wiley*. DOI: 10.1002/9781118476406.emoe536

White, D.J. and Randolph, M.F. (2007). Seabed characterisation and models for pipeline-soil interaction. *Int. Journal of Offshore & Polar Engng*. **17**(3):193–204

White, D.J. (2020). Modern Geotechnical Centrifuge Modelling. *Chapter in Physical Models in Civil and Building Engineering: Their History and Current Use, Wiley*. Ed. Addis, Kurrer & Lorenz. Chapter 34, pp965-984 https://doi.org/10.1002/9783433609613.ch34

White, D., Bruton, D. A. S., Bolton, M., Hill, A. J., Ballard, J.-C., and Langford, T. (2011). SAFEBUCK JIP - Observations of Axial Pipe- soil Interaction from Testing on Soft Natural Clays. Offshore Technology Conference.

White, D.J., Clukey, E.C., Randolph, M.F., Boylan, N.P., Bransby, M.F., Zakeri, A., Hill, A.J. and Jaeck, C. (2017). The state of knowledge of pipe-soil interaction for on-bottom pipeline design. OTC 27623, Proc. Offshore Technology Conference, Houston.

Yan, Y., White, D.J. and Randolph, M.F. (2014). Cyclic consolidation and axial friction on seabed pipelines Geotechnique Letters **4**:165–169